surface and tear function differences between these two types of dry eye.

Patients and methods

Patients

Fifty eyes of 25 patients who underwent HSCT were enrolled at the dry eye clinic at Keio University from January 2006 to December 2006. Included were 20 eyes of 10 patients (5 males and 5 females; range, 30–66; median, 50 years) with cGVHD-related severe dry eye, 20 eyes of 10 patients (6 males and 4 females; range, 37–62; median, 51 years) with cGVHD-related mild dry eye and 10 eyes of 5 patients (3 males and 2 females; range, 39–50; median, 45 years) without dry eye. All the patients had no previous conjunctival or corneal disease or infections or other ocular disease at clinical examination. Twenty-eight eyes of 14 healthy subjects (10 males and 4 females; range, 20–70; median, 39 years) were also recruited as normal controls. The control subjects did not have any history of ocular or systemic disease or a history of topical eye drops or contact lens use that would alter the ocular surface as well. According to the global diagnostic criteria of dry eye, and the severity grading of the Dry Eye Workshop Report 2007,[11,12] we diagnosed the patients as having dry eye when patients had any sign of tear film instability (tear break-up time (BUT) $\leqslant$5 s, Schirmer test $\leqslant$5 mm), any abnormality of the ocular surface (Rose Bengal score $\geqslant$3, Fluorescein score $\geqslant$1) and/or symptoms of ocular irritation. Severe dry eye was defined as previously described[2,13] In brief, patients were diagnosed as having severe dry eye if the Schirmer test with nasal stimulation (reflex tearing) was $\leqslant$10 mm, and the FS and RB scores were $\geqslant$3 points and/or grade 3 and 4 according to the DEWS report 2007. The study was carried out in accordance with the principles of the Declaration of Helsinki. Informed consents and ethics board reviews for the examination procedure were obtained.

Clinical examinations

The ocular surface was examined by the double vital staining method. Two microliters of a preservative-free combination of 1% Rose Bengal and 1% fluorescein was instilled in the conjunctival sac by a micropipette.[14] The staining of Rose Bengal was scored for the temporal and nasal conjunctiva and the cornea, on a scale of 0–3 points. Fluorescein staining score also ranged between 0 and 9 points, but only for the cornea.[15] The BUT value was measured three times at the time of double staining, and the mean value was used for calculation. Schirmer 1 test was performed with standardized strips of filter paper (Alcon Inc., Fort Worth, TX, USA). To evaluate the obstruction of the MG orifice, digital pressure was applied on the tarsus. The expression of meibomian secretion (meibum) was scored as follows:[16] grade 0, clear meibum is easily expressed; grade 1, cloudy meibum is expressed with mild pressure; grade 2, cloudy meibum is expressed with more than moderate pressure; and grade 3, meibum cannot be expressed even with hard pressure.

Tear evaporimetry

The tear evaporation was measured with the evaporimeter (KAO Corporation, Tokyo, Japan).[17] Briefly, the eyecup of the evaporimeter tightly covered the subject's eye, and then the device measured the tear evaporation rate in both eyes-closed and eyes-open conditions. In this way, we can eliminate the evaporation from the eyelid. The computer system calculated the difference between these two conditions and gave the tear evaporation rate. The unit of tear evaporation rate is 10^{-7} g/cm^{2}s.

Corneal sensitivity

Measurement of corneal sensitivity (CS) was performed using a Cochet-Bonnet aesthesiometer. The measurements were begun with the nylon filament fully extended. The tip of the nylon filament was applied perpendicularly to the surface of the cornea making certain not to touch the eyelashes and was pushed until the fiber's first visible bending. The length of the fiber was gradually decreased until a blink reflex was observed. The length was recorded in units of millimeters. Measurements were taken from the central cornea and the mean of the measurements was recorded as the CS reading of that eye.[18,19]

Conjunctival impression cytology

The impression cytology samples were obtained under topical anesthesia with 0.4% oxybuprocaine. A piece of cellulose acetate filter paper (Millipore HAWP 304, Bedford, MA, USA) was put on the temporal bulbar conjunctiva and gently pressed by forceps for several seconds. The specimens were fixed with 10% formalin neutral buffer solution and stained with Periodic Acid-Schiff (PAS). Five nonoverlapping areas of $\times$400 magnification were randomly selected and photographed. The goblet cell density (GCD) was reported as cells per square millimeter. The conjunctival epithelial squamous metaplasia was evaluated according to Nelson's grading scheme.[20]

Conjunctival brush cytology

The brush cytology samples were collected after administration of topical anesthesia with 0.4% oxybuprocaine. The central upper palpebral conjunctiva was gently brushed seven times with a disposable dental brush 1.5 mm in diameter (Dentalpro, Jacks. Co., Osaka, Japan). After sampling, the brush was immediately put in 1 ml of Hank's solution and shaken several times to detach the cells from the brush. The suspended cells were centrifuged with cytocentrifuge at 700 r.p.m. for 10 min to make the monolayer cell smears. The slides were stained by diff-quick staining. We counted up to 500 cells including inflammatory cells and epithelial cells in nonoverlapping fields under microscopic observation (magnification, $\times$400). The inflammation was reported as the number of inflammatory cells in the total number of 500 brush cells.[19]

Statistical analysis

The data were analyzed by Instat (GraphPad Software, San Diego, CA, USA). Mann–Whitney *U*-test was used to compare the onset duration of dry eye. Kruskal–Wallis *H*-test

was used for the comparisons of clinical examination parameters, tear evaporation rates, GCD, conjunctival squamous metaplasia, and inflammatory cell amount. The probability level of 5% was chosen as the statistical significance.

Results

Demographic characteristics

Patients' demographic characteristics were summarized in Table 1. The onset of dry eye in cGVHD-related severe and mild dry eye was 6.8 ± 2.5 and 13.2 ± 9.1 months, respectively, after HSCT. The onset of dry eye in the severe dry eye group was significantly earlier than the onset in the mild dry eye group ($P = 0.02$). Nine out of 10 severe dry eye patients had systemic cGVHD, but only 3 in 10 mild dry eye patients had systemic cGVHD.

Clinical examination parameters

The baseline scores of CS, ocular surface vital staining and tear function were summarized in Table 2. Obviously decreased CS was found in post-HSCT patients either with or without dry eye, but statistically significant decrease was found only in the severe dry eye group. Although the mean CS in the severe dry eye group was considerably lower than those with mild dry eye and post-HSCT without the dry eye groups, there was no statistically significant difference among the three groups. Obvious MG orifice obstruction (grade >1) was noted in 40 of 50 eyes of the post-HSCT patients as shown in Table 3. MG orifice obstruction degree in post-HSCT patients was statistically higher than normal controls, but there was no significant difference between the three post-HSCT groups. The tear evaporation rate in normal control, post-HSCT without dry eye, mild dry eye, and severe dry eye group was $2.2 \pm 1.53 \times 10^{-7}$ g/cm^{2}s, $4.42 \pm 2.13 \times 10^{-7}$, $3.6 \pm 1.66 \times 10^{-7}$,

Table 1 Demographic characteristics

Case no	*Age (years)*	*Gender*	*Diagnosis*	*Systemic cGVHD*	*Dry eye*	*Onset (month from HSCT to dry eye)*	*Month since HSCT*
1	52	M	MDS	Lung, skin, mouth	Severe	7	29
2	63	M	MDS	Liver, skin, mouth	Severe	6	65
3	64	M	MM	Skin, mouth	Severe	7	30
4	35	F	CML	Mouth	Severe	7	61
5	30	F	AML	Mouth	Severe	7	93
6	50	M	AML	Mouth, skin, liver	Severe	3	69
7	36	M	CML	Mouth	Severe	7	88
8	66	F	MM	Mouth, skin	Severe	11	58
9	57	F	MDS	Mouth, skin	Severe	10	34
10	34	F	ALL	(−)	Severe	3	144
11	49	M	ALL	Lung, liver, skin	Mild	9	24
12	54	M	ALL	Mouth, skin, intestinal	Mild	12	66
13	59	F	ALL	(−)	Mild	11	96
14	56	M	MDS	Liver	Mild	36	156
15	62	F	ALL	(−)	Mild	2.5	19
16	37	M	MDS	(−)	Mild	5	28
17	45	M	MDS	(−)	Mild	12	12
18	61	F	ALL	(−)	Mild	16	36
19	51	M	AML	(−)	Mild	15	36
20	58	F	NHL	(−)	Mild	13	30
21	45	M	AA	(−)	(−)	(−)	60
22	44	F	AML	(−)	(−)	(−)	120
23	39	F	CML	(−)	(−)	(−)	144
24	50	M	AML	(−)	(−)	(−)	30
25	48	M	AML	(−)	(−)	(−)	3

Abbreviations: AA = aplastic anemia; cGVHD = chronic GVHD; F = female; HSCT = hematopoietic stem cell transplantation; M = male; MDS = myelodysplastic syndrome; MM = multiple myeloma; NHL = non-Hodgkin lymphoma.

Table 2 The scores of tear functions, corneal sensitivity and vital stainings

	Tear evaporation rate ($\times 10^{-7}$ g/cm^2 s)	*CS (mm)*	*Schirmer test (mm)*	*BUT (s)*	*FS (points)*	*RB (points)*
Normal controls	2.2 ± 1.53	60	16.35 ± 11.82	8.92 ± 3.17	0.54 ± 0.66	0.13 ± 0.34
Post-HSCT without dry eye	4.42 ± 2.13	57.5 ± 4.63	14.7 ± 10.34	10	0.3 ± 0.95	0.3 ± 0.95
cGVHD-related mild dry eye	3.6 ± 1.66	57.25 ± 4.16	13.06 ± 11.05	$4.85 \pm 2.18^{a,b}$	$2.4 \pm 1.93^{a,b}$	1.8 ± 1.85^{a}
cGVHD-related severe dry eye	5.98 ± 3.61^{a}	54.98 ± 7.75^{a}	$2.45 \pm 2.28^{a,b,c}$	$2.68 \pm 1.4^{a,b}$	$5.6 \pm 2.56^{a,b,c}$	$5.55 \pm 2.06^{a,b,c}$

Abbreviations: BUT = tear break-up time; cGVHD = chronic GVHD; FS = fluorescein score; HSCT = hematopoietic stem cell transplantation; RB = Rose Bengal score.

[a] $P < 0.05$, compared with normal controls, Kruskal–Wallis test.

[b] $P < 0.05$, compared with post-HSCT without dry eye patients, Kruskal–Wallis test.

[c] $P < 0.05$, compared with cGVHD-related mild dry eye patients, Kruskal–Wallis test.

Table 3 Comparison of orifice obstruction grade of meibomian gland

Orifice obstruction	*Normal controls*	*Post-HSCT without dry eye*	*cGVHD-related mild dry eye*	*cGVHD-related severe dry eye*
Grade 0	26 (92.86%)	2 (20%)	0	2 (10%)
Grade 1	2 (7.14%)	2 (20%)	4 (20%)	0
Grade 2	0	2 (20%)	7 (35%)	5 (25%)
Grade 3	0	4 (40%)	9 (45%)	13 (65%)

Abbreviations: cGVHD = chronic GVHD; HSCT = hematopoietic stem cell transplantation.

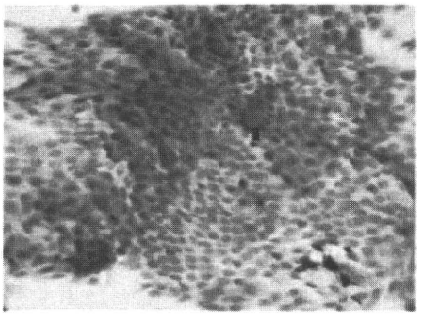

Figure 1 Representative conjunctival impression cytology specimens from a 50-year-old male, post-HSCT without dry eye subject. Note plenty goblet cells (black arrow) and mucin pick up (yellow arrows). Periodic acid-Schiff (PAS) staining, magnification, × 400.

and $5.98 \pm 3.61 \times 10^{-7}$ g/cm^{2}s, respectively. Although the mean tear evaporation rate in mild dry eye and post-HSCT without dry eye patients was higher than in normal controls, statistically increased tear evaporation was found only in cGVHD-related severe dry eye patients ($P<0.001$).

Conjunctival impression cytology

Conjunctival specimens from normal controls and post-HSCT without dry eye subjects showed plenty of goblet cells and mucin pick up (Figure 1). The goblet cell densities in these two groups were 1313.13 ± 733.82 and 1030 ± 433.14 cells/mm^2. The mean GCD in the cGVHD-related mild and severe dry eye groups was 706.49 ± 583.52 and 396.36 ± 381.00 cells/mm^2. Both were obviously lower than the former two groups without dry eye (Table 4). Moreover, significant conjunctival epithelial squamous metaplasia was noted in severe dry eye patients. The mean grades of squamous metaplasia in normal control, post-HSCT without dry eye, and mild dry eye groups were 0.70 ± 0.46, 0.71 ± 0.52, and 0.72 ± 0.56, respectively. There was no statistical difference among the three groups. However, the average grade of squamous metaplasia in severe dry eye subjects was 1.61 ± 0.72, which was significantly higher than that in the other three groups (Table 4). Except decreased GCD, the PAS staining also showed inflammation in some impression cytology specimens from the cGVHD-related severe dry eye and mild dry eye patients (Figures 2 and 3). In addition, the PAS staining also indicated the intense inflammatory cell infiltration that frequently appeared with the abnormal mucin conglomeration.

Brush cytology

There was no inflammatory cell in the brush cytology specimens from normal controls. In contrast, a different extent of inflammatory cell infiltration was found in the specimens from post-HSCT patients (Figure 4). The mean number of inflammatory cells in 500 brush cells in post-HSCT without dry eye, mild dry eye, and severe dry eye specimens were 5.44 ± 6.04 cells, 14.64 ± 9.75 cells, and 22.64 ± 11.69 cells, respectively. The mean inflammatory cell numbers in both cGVHD-related mild and severe dry eye specimens were significantly higher than in normal controls and post-HSCT without the dry eye group ($P<0.001$). Moreover, the inflammatory cell number in the severe dry eye group was statistically higher than in the mild dry eye group ($P-0.03$).

Discussion

In this study, we evaluated the detailed baseline profiles of ocular surface and tear function alterations in post-HSCT patients with or without dry eye disease. We found obviously decreased CS in post-HSCT subjects either with or without dry eye disease. Although the reduction of CS in severe dry eye patients seemed to be more prominent, there were no statistical differences compared with post-HSCT without dry eye and mild dry eye patients. A reduction of CS has been reported in dry eye patients.[18,19] We also noted decreased CS in cGVHD-related dry eye patients in our previous study.[3] Considering the conditioning regimens before HSCT, such as total body irradiation, which includes orbital irradiation, we thought decreased CS in cGVHD-related dry eye patients may not be because of the dry eye pathologic process. Therefore, we recruited post-HSCT without dry eye subjects in this study. According to the present results, decreased CS was obvious even in post-HSCT without dry eye patients. Our study suggested that the conditioning regimens before HSCT may be more responsible for the decreased CS in cGVHD-related dry eye disease.

Moreover, increased MG obstruction grade was found in post-HSCT both with and without dry eye patients. Consistent with this, an increased tendency in the tear evaporation rate was noted in post-HSCT patients. However, the statistical increase was found only in the severe dry eye patients. MGs produce lipid material that spread and cover the ocular surface during the blink to keep the tear film stable and to reduce the tear evaporation. The dysfunction of the MG can induce evaporative dry eye.[21] On the other hand, decreased tear production

Table 4 Comparison of conjunctival GCD and epithelium squamous metaplasia

	Normal controls	*Post-HSCT without dry eye*	*cGVHD-related mild dry eye*	*cGVHD-related severe dry eye*
GCD (cells/mm^2)	1313.13 ± 733.82	1030 ± 433.14	706.49 ± 583.52[a]	396.36 ± 381.00[a,b]
Squamous metaplasia (Nelson's)	0.70 ± 0.46	0.71 ± 0.52	0.72 ± 0.56	1.61 ± 0.72[a,b,c]

Abbreviations: cGVHD = chronic GVHD; GCD = goblet cell density; HSCT = hematopoietic stem cell transplantation.
[a]$P<0.05$, compared with normal controls, Kruskal Wallis test.
[b]$P<0.05$, compared with post-HCT without dry eye patients, Kruskal Wallis test.
[c]$P<0.05$, compared with cGVHD-related mild dry eye patients, Kruskal Wallis test.

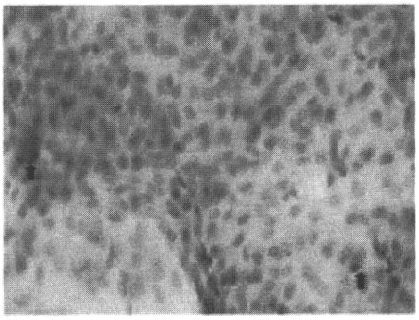

Figure 2 Representative conjunctival impression cytology specimens from a 37-year-old male, cGVHD-related mild dry eye patient. Note decreased goblet cell number (black arrow), and the conjunctival epithelium has no obvious keratinization. Periodic acid-Schiff (PAS) staining, magnification, × 400.

can also cause an increase in the tear evaporation rate.[22] Taken together, these findings suggest that increased MGD in post-HSCT patients cause enhanced tear evaporation in both groups of patients with or without dry eye, and enhanced tear evaporation acting together with the decreased tear production, induced the enhancement of ocular surface changes and tear function changes in cGVHD-related severe dry eye patients.

In our previous study,[2] we noticed the fact that there were two types of dry eye after HSCT. One had severe ocular surface and tear function alterations with decreased reflex tearing, which occurred soon after the onset of dry eye. Another was mild with normal reflex tearing. In this study, we performed a further comparison about the difference between these two types of dry eye. We found that the onset of cGVHD-related severe dry eye was obviously earlier than that of mild dry eye. In our patients, severe dry eye occurred around 6.8 ± 2.5 months after HSCT, but the onset of mild dry eye was around 13.2 ± 9.1 months after HSCT. There was one patient in whom the mild dry eye occurred 3 years after the HSCT. Moreover, most severe dry eye patients had systemic cGVHD, whereas only a few patients in the mild dry group had systemic cGVHD. Those findings indicated the different pathologic processes in cGVHD-related severe and mild dry eye disease.

For further comparison, we performed conjunctival impression cytology to evaluate the alterations and differences in GCD and squamous metaplasia in these two types of dry eye disease. GCD and squamous metaplasia are two parameters that were widely used to evaluate the ocular surface epithelial condition in dry eye and other ocular surface disease.[18,23,24] In addition, goblet cell content has been reported to be a sensitive indicator of primary ocular surface disease.[25,26] However, the report concerning the conjunctival impression cytology characteristics in cGVHD-related dry eye disease was still rare.[8] In this study, we found that both cGVHD-related mild and severe dry eye specimens showed significantly decreased GCD compared with normal controls and post-HSCT without dry eye specimens. Moreover, the mean GCD in severe dry eye patients was only about half of the density in mild dry eye patients with decrease in goblet cell numbers along with increased squamous metaplasia and keratinization of the ocular surface.[27] In cGVHD-related mild dry eye, although the GCD decreased, there was no obvious squamous metaplasia. However, high grades of squamous metaplasia with a further decrease in goblet cell numbers were found in severe dry eye patients. On the basis of these findings, we confirmed GCD to be a sensitive indicator for evaluating the extent of cGVHD-related dry eye disease. Except for decreased GCD and squamous metaplasia, some impression cytology specimens from cGVHD-related dry eye patients showed inflammatory cell infiltration in the conjunctival epithelium. These intense inflammatory areas often appeared in the area with clustered abnormal mucin. It indicates that the inflammation process involves the pathologic changes of cGVHD-related dry eye, which may influence the secretion and physiological characteristics of the ocular surface mucin.

For revealing the inflammation status in cGVHD-related dry eye disease and comparing the inflammation extent between cGVHD-related severe and mild dry eye disease, we collected the conjunctival brush cytology specimens and calculated the amount of inflammatory cells. We found considerably increased inflammatory cell numbers in both cGVHD-related severe dry eye and mild dry eye patients compared with normal controls and post-HSCT without dry eye subjects. Moreover, the number of inflammatory cells in severe dry eye specimens was significantly higher than in mild dry eye specimens. Recently, increased evidence suggests that dry eye is an inflammation-related disease.[28] Our previous study also found many inflammatory markers expressed in biopsy samples of the conjunctiva and lacrimal gland from cGVHD-related dry eye patients.[4,6] The present findings confirm that inflammation is involved in the pathogenesis of cGVHD-related dry eye. Moreover, our results suggest that the extent of

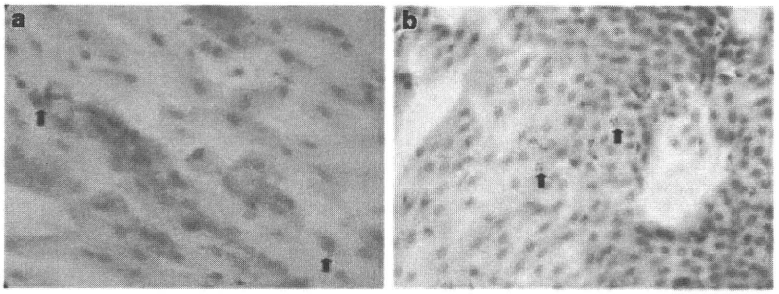

Figure 3 Representative conjunctival impression cytology specimens from a 52-year-old male cGVHD-related severe dry eye patient. (**a**) Note obvious squamous meterplasia and decreased GCD. Black arrows indicate the small goblet cells with decreased cytoplasmic mucin. (**b**) Note inflammatory infiltration (black arrows) in the conjunctival epithelium. Periodic acid-Schiff (PAS) staining, magnification, ×400.

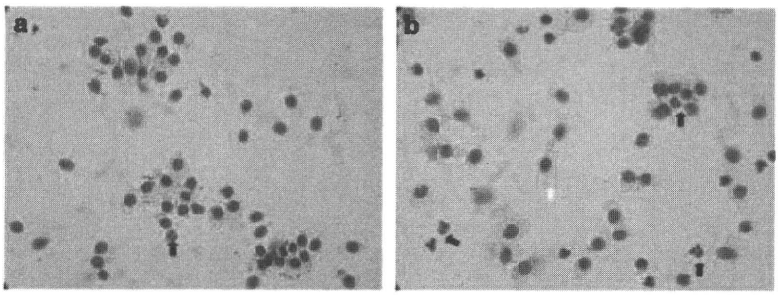

Figure 4 Representative brush cytology (BC) specimens. (**a**) Specimen from a 37-year-old male, cGVHD-related mild dry eye patient. Note inflammatory cells (black arrow). (**b**) Specimen from a 66-year-old female cGVHD-related severe dry eye patient. Note obviously inflammatory cells (black arrows) and keratinized conjunctival epithelial cells (yellow arrow). Diff-quick staining, magnification, ×400.

inflammation may be responsible for the different extent of pathologic damage in cGVHD-related mild and severe dry eye disease.

As the time we collected the brush cytology and impression cytology samples was relatively far from the onset of the dry eye, it is hard to distinguish whether the inflammation is the consequence or a cause of cGVHD-related dry eye. However, these two techniques are relatively noninvasive and repeatable examinations. They are very suitable to monitor the dynamic changes of the ocular surface epithelium and inflammation after HSCT. Moreover, the impression cytology and brush cytology samples can also be used to perform immunohistochemical staining, enzyme-linked immunosorbent assay, flow cytometry, and mRNA expression analysis.[9,10,29,30] Therefore, they are also useful to monitor the pathologic progress in cGVHD-related dry eye disease and helpful for investigating the etiology of cGVHD-related dry eye disease.

In this study, we used the tear evaporimetry, MG expression examination, impression cytology, and brush cytology to give a comprehensive evaluation of the changes of ocular surface and tear functions in patients with cGVHD-related mild and severe dry eye disease, and compared the results with healthy controls and post-HSCT patients without dry eye disease. According to the findings in this study, we speculated that the extent of the inflammatory process seems to have a pivotal role in the outcome of cGVHD-related dry eye disease with changes in tear evaporation, CS and GCD acting as determinants of the differences of the ocular surface healthy status.

In conclusion, our present data provide the baseline data of each type of dry eye disease associated with cGVHD using these methods. These data are also useful for future therapeutic evaluation.

Conflict of interest

The authors declare no conflict of interest.

Acknowledgements

This work was presented in part at the 60th Japan Congress of Clinical Ophthalmology, 5–8 October 2006, Kyoto, Japan and ARVO 2007, Fort Lauderdale, USA. This work was supported by a grant from the Japanese Ministry of Education, Science, Sports and Culture #20592058.

References

1 Filipovich AH, Weisdorf D, Pavletic S, Socie G, Wingard JR, Lee SJ *et al.* National Institutes of Health consensus development project on criteria for clinical trials in chronic

graft-versus-host disease: I. Diagnosis and staging working group report. *Biol Blood Marrow Transplant* 2005; **11**: 945 956.
2 Ogawa Y, Okamoto S, Wakui M, Watanabe R, Yamada M, Yoshino M *et al.* Dry eye after hematopoietic stem cell transplantation. *Br J Ophthalmol* 1999; **83**: 1125 1130.
3 Ogawa Y, Okamoto S, Mori T, Yamada M, Mashima Y, Watanabe R *et al.* Autologous serum eye drops for the treatment of severe dry eye in patients with chronic graft-versus-host disease. *Bone Marrow Transplant* 2003; **31**: 579 583.
4 Ogawa Y, Yamazaki K, Kuwana M, Mashima Y, Nakamura Y, Ishida S *et al.* A significant role of stromal fibroblasts in rapidly progressive dry eye in patients with chronic GVHD. *Invest Ophthalmol Vis Sci* 2001; **42**: 111 119.
5 Ogawa Y, Kuwana M, Yamazaki K, Mashima Y, Yamada M, Mori T *et al.* Periductal area as the primary site for T-cell activation in lacrimal gland chronic graft-versus-host disease. *Invest Ophthalmol Vis Sci* 2003; **44**: 1888 1896.
6 Rojas B, Cuhna R, Zafirakis P, Ramirez JM, Lizan-garciia M, Zhao T *et al.* Cell populations and adhesion molecules expression in conjunctiva before and after bone marrow transplantation. *Exp Eye Res* 2005; **81**: 313 325.
7 Singh R, Joseph A, Umapathy T, Tint NL, Dua HS. Impression cytology of the ocular surface. *Br J Ophthalmol* 2005; **89**: 1655 1659.
8 Dogru M, Okada N, Asano-Kato N, Tanaka M, Igarashi A, Takano Y *et al.* Atopic ocular surface disease: implications on tear function and ocular surface mucins. *Cornea* 2005; **24**: S18 S23.
9 Miyoshi T, Fukagawa K, Shimmura S, Fujishima H, Takano Y, Takamura E *et al.* Interleukin-8 concentrations in conjunctival epithelium brush cytology samples correlate with neutrophil, eosinophil infiltration, and corneal damage. *Cornea* 2001; **20**: 743 747.
10 Aronni S, Cortes M, Sacchetti M, Lambiase A, Micera A, Sgrulletta R *et al.* Upregulation of ICAM-1 expression in the conjunctiva of patients with chronic graft-versus-host disease. *Eur J Ophthalmol* 2006; **16**: 17 23.
11 Lemp MA. Report of the national eye institute/industry workshop on clinical trials in dry eyes. *CLAO J* 1995; **21**: 221 232.
12 Report of the International Dry Eye Work Shop. *Ocul Surf* 2007; **5**: 75 92.
13 Tsubota K. The importance of the Schirmer test with nasal stimulation test. *Am J Ophthalmol* 1991; **111**: 106 108.
14 Toda I, Tsubota K. Practical double vital staining for ocular surface evaluation. *Cornea* 1993; **12**: 366 368.
15 Dogru M, Asano-Kato N, Tanaka M, Igarashi A, Shimmura S, Shimazaki J *et al.* Ocular surface and MUC5AC alterations in atopic patients with corneal shield ulcers. *Curr Eye Res* 2005; **30**: 897 908.
16 Shimazaki J, Goto E, Ono M, Shimmura S, Tsubota K. Meibomian gland dysfunction in patients with Sjogren syndrome. *Ophthalmology* 1998; **105**: 1485 1488.
17 Goto E, Endo K, Suzuki A, Fujikura Y, Matsumoto Y, Tsubota K. Tear evaporation dynamics in normal subjects and subjects with obstructive meibomian gland dysfunction. *Invest Ophthalmol Vis Sci* 2003; **44**: 533 539.
18 Xu KP, Yagi Y, Tsubota K. Decrease in corneal sensitivity and change in tear function in dry eye. *Cornea* 1996; **15**: 235 239.
19 Bourcier T, Acosta MC, Borderie V, Borrás F, Gallar J, Bury T *et al.* Decreased corneal sensitivity in patients with dry eye. *Invest Ophthalmol Vis Sci* 2005; **46**: 2341 2345.
20 Nelson JD. Impression cytology. *Cornea* 1988; 7: 71 81.
21 McCulley JP, Shine WE. The lipid layer of tears: dependent on meibomian gland function. *Exp Eye Res* 2004; **78**: 361 365.
22 Mathers W. Evaporation from the ocular surface. *Exp Eye Res* 2004; **78**: 389 394.
23 Tseng SC. Staging of conjunctival squamous metaplasia by impression cytology. *Ophthalmology* 1985; **92**: 728 733.
24 Aragona P, Ferreri G, Micali A, Puzzolo D. Morphological changes of the conjunctival epithelium in contact lens wearers evaluated by impression cytology. *Eye* 1998; **12**: 461 466.
25 Tseng SC, Hirst LW, Maumenee AE, Kenyon KR, Sun TT, Green WR. Possible mechanisms for the loss of goblet cells in mucin-deficient disorders. *Ophthalmology* 1984; **91**: 545 552.
26 Kinoshita S, Kiorpes TC, Friend J, Thoft RA. Goblet cell density in ocular surface disease. A better indicator than tear mucin. *Arch Ophthalmol* 1983; **101**: 1284 1287.
27 Gipson IK, Hori Y, Argueso P. Character of ocular surface mucins and their alteration in dry eye disease. *Ocul Surf* 2004; **2**: 131 147.
28 Stern ME, Pflugfelder SC. Inflammation in dry eye. *Ocul Surf* 2004; **2**: 124 130.
29 Tsubota K, Fujihara T, Saito K, Takeuchi T. Conjunctival epithelium expression of HLA-DR in dry eye patients. *Ophthalmologica* 1999; **213**: 16 19.
30 Rolando M, Barabino S, Mingari C, Moretti S, Giuffrida S, Calabria G. Distribution of conjunctival HLA-DR expression and the pathogenesis of damage in early dry eyes. *Cornea* 2005; **24**: 951 954.

Alloantigen expression on non-hematopoietic cells reduces graft-versus-leukemia effects in mice

Shoji Asakura,[1] Daigo Hashimoto,[1,2] Shuichiro Takashima,[3] Haruko Sugiyama,[1] Yoshinobu Maeda,[1] Koichi Akashi,[2,3] Mitsune Tanimoto,[1] and Takanori Teshima[2]

[1]Biopathological Science, Okayama University Graduate School of Medicine and Dentistry, Okayama, Japan. [2]Center for Cellular and Molecular Medicine and [3]Department of Medicine and Biosystemic Science, Kyushu University Graduate School of Science, Fukuoka, Japan.

Allogeneic hematopoietic stem cell transplantation (HSCT) is used effectively to treat a number of hematological malignancies. Its beneficial effects rely on donor-derived T cell–targeted leukemic cells, the so-called graft-versus-leukemia (GVL) effect. Induction of GVL is usually associated with concomitant development of graft-versus-host disease (GVHD), a major complication of allogeneic HSCT. The T cells that mediate GVL and GVHD are activated by alloantigen presented on host antigen-presenting cells of hematopoietic origin, and it is not well understood how alloantigen expression on non-hematopoietic cells affects GVL activity. Here we show, in mouse models of MHC-matched, minor histocompatibility antigen–mismatched bone marrow transplantation, that alloantigen expression on host epithelium drives donor T cells into apoptosis and dysfunction during GVHD, resulting in a loss of GVL activity. During GVHD, programmed death–1 (PD-1) and PD ligand–1 (PD-L1), molecules implicated in inducing T cell exhaustion, were upregulated on activated T cells and the target tissue, respectively, suggesting that the T cell defects driven by host epithelial alloantigen expression might be mediated by the PD-1/PD-L1 pathway. Consistent with this, blockade of PD-1/PD-L1 interactions partially restored T cell effector functions and improved GVL. These results elucidate a previously unrecognized significance of alloantigen expression on non-hematopoietic cells in GVL and suggest that separation of GVL from GVHD for more effective HSCT may be possible in human patients.

Introduction

Donor immunity in allogeneic hematopoietic stem cell transplantation (HSCT) harnesses beneficial graft-versus-leukemia (GVL) effects; therefore, allogeneic HSCT represents a very potent form of immunotherapy for hematological malignancies (1, 2). Induction of GVL is usually associated with the development of graft-versus-host disease (GVHD), which is a major complication after allogeneic HSCT. T cell depletion of the donor inocula prevents GVHD and leads to a loss of the GVL effect (3–5). Both GVL and GVHD are mediated by donor T cells, which recognize alloantigens presented on host APCs (6, 7). Donor CTLs and inflammatory cytokines are major effectors of GVHD, whereas CTLs are primarily responsible for GVL (8, 9). In patients with advanced-stage leukemia and lymphoma, relapse is still a major cause of mortality after allogeneic HSCT even after the development of severe GVHD. Thus, improvements in our understanding of the pathophysiology of GVHD and GVL are urgently needed to develop more effective therapies for malignant diseases.

Alloantigens are expressed on the three major components in HSCT recipients in the context of GVHD and GVL: hematopoietically derived APCs, GVHD target epithelium, and leukemia cells. Several studies have shown that host APCs are crucial for the induction of both GVHD and GVL (6, 7, 9–11). Alloantigen expression on epithelium is also critical for the induction of GVHD in MHC-matched, minor histocompatibility antigen–mismatched (mHA-mismatched) models of bone marrow transplantation (BMT) (10), but GVHD can occur in the absence of alloantigen expression on epithelium in MHC-mismatched models of BMT (9). However, the effect of alloantigen expression on non-hematopoietic cells such as the epithelium in GVL is not well defined. In this study, we addressed this important issue in mHA-mismatched models of BMT.

Results

Alloantigen expression on host non-hematopoietic cells augments acute GVHD but reduces GVL effects. We generated BM chimeric mice that express alloantigens on APCs, which are essential for the induction of both GVHD and GVL (6, 7, 12). BM chimeras were created by reconstituting lethally irradiated C3H.Sw (C3: H-2^b) mice with 5×10^6 T cell–depleted (TCD) BM cells isolated from C57BL/6 (B6, H-2^b) mice that differ from C3 mice at multiple mHAs ([B6→C3] chimeras). Control chimeras, [B6→B6], were identically created. Four months later, donor repopulation of hematopoiesis was confirmed by flow cytometry as shown previously (6, 9, 12). Thus, [B6→C3] chimeric mice expressed B6-derived mHAs on hematopoietically derived APCs but not on non-hematopoietic target cells. In contrast, [B6→B6] mice expressed B6-derived mHAs on both APCs and target epithelium. These chimeras were used as BMT recipients; they were reirradiated and injected with 5×10^6 TCD BM cells alone or with various doses of $CD8^+$ T cells from C3 donors. After BMT, GVHD mortality was higher in [B6→B6] mice than in [B6→C3] mice (Figure 1A). Clinical GVHD scores (13) in surviving animals were also higher in [B6→B6] mice than in [B6→C3] mice (Figure 1B). Mortality and morbidity from GVHD in [B6→C3] mice were almost equivalent to those in [B6→B6] mice given a 1-log lower T cell dose. This finding confirmed the previous observation of a lack of alloantigen expression on host epithelium significantly reducing GVHD across mHA disparity (10). We

Conflict of interest: The authors have declared that no conflict of interest.

Citation for this article: *J Clin Invest.* 2010;120(7):2370–2378. doi:10.1172/JCI39165.

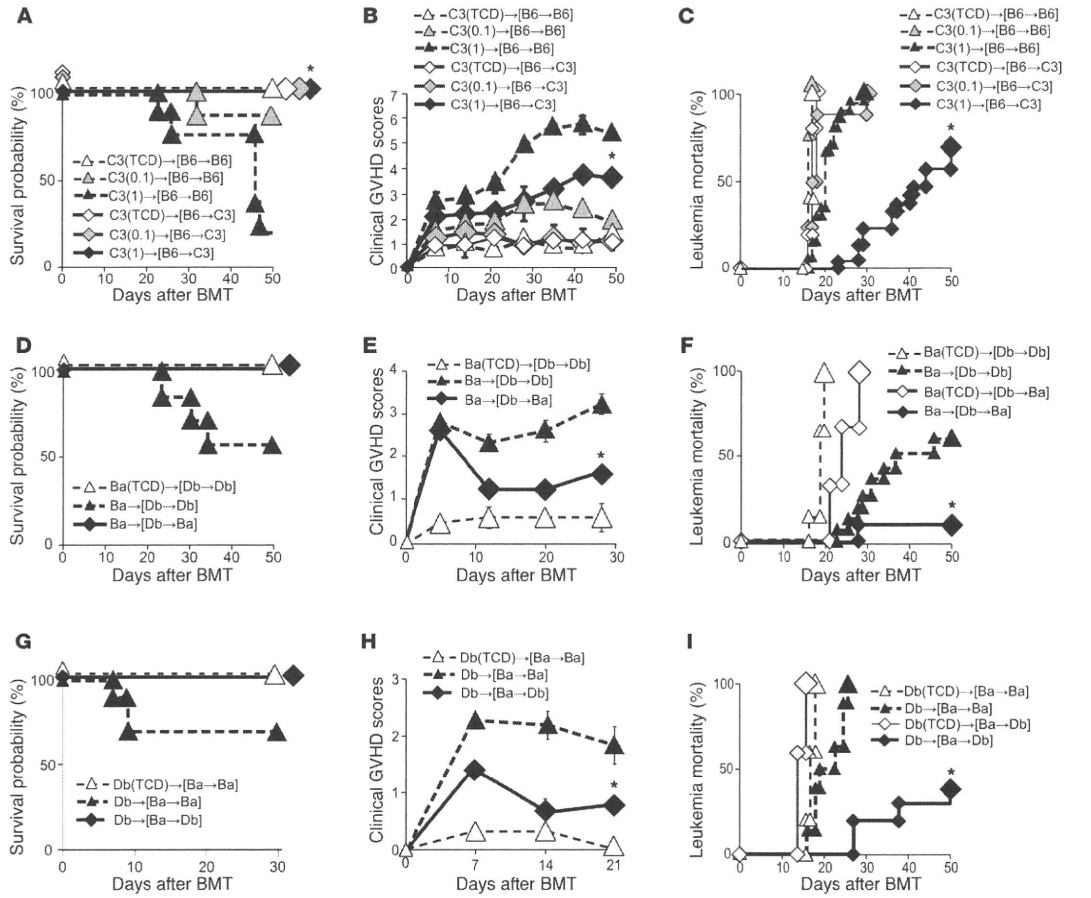

Figure 1

Alloantigen expression on host non-hematopoietic cells augments acute GVHD but reduces GVL effects. (**A–C**) [B6→C3] (diamonds) and [B6→B6] chimeras (triangles) were created by reconstituting lethally irradiated C3 and B6 mice with 5×10^6 TCD BM cells from B6 mice. Four months later, the chimeras were reirradiated and injected with 5×10^6 TCD BM cells alone (open symbols) or with 1×10^6 (black symbols) or 0.1×10^6 (gray symbols) CD8$^+$ T cells from C3 donors (as indicated in parentheses $\times 10^6$). Survival (**A**) and clinical GVHD scores (**B**) after BMT (n = 3–8/group). (**C**) Leukemia mortality after BMT in chimeras injected with EL4 cells (n = 5–21/group). Data from 3 similar experiments were combined. (**D–F**) [Db→Ba] (diamonds) and [Db→Db] (triangles) chimeras were reirradiated and injected with TCD BM alone (open symbols) or with 2×10^6 T cells from Ba donors (filled symbols). Survival (**D**) and clinical GVHD scores (**E**) after BMT from a representative experiment of 2 similar experiments (n = 4–7/group). (**F**) Leukemia mortality after BMT in mice injected with P815 cells. Data from 2 similar experiments were combined (n = 6–18/group). (**G–I**) [Ba→Db] (diamonds) and [Ba→Ba] (triangles) chimeras were similarly transplanted with 5×10^6 TCD BM cells alone (open symbols) or with 2×10^6 T cells from Db donors (filled symbols). Survival (**G**) and clinical scores (**H**) after BMT (n = 3–10/group). (**I**) Leukemia mortality after BMT in chimeras injected with A20 cells (n = 5–10/group). Data from 2 similar experiments were combined. Clinical scores are shown as the mean ± SEM. *$P < 0.05$ compared with allogeneic controls.

then tested the effect of alloantigen expression on GVHD target epithelium on GVL effects. These chimeric mice were transplanted as described above together with 2,500 B6-derived EL4 cells as a model of residual leukemia after BMT. As expected, 100% of both types of chimeric mice that received TCD BM cells died from leukemia by day +20 after BMT (Figure 1C), whereas leukemia-free survival was significantly prolonged in mice that received donor T cells, demonstrating a significant GVL effect. However, this GVL effect was not potent in [B6→B6] mice, and all mice subsequently died from leukemia. Surprisingly, leukemia mortality was significantly lower in [B6→C3] mice that did not express alloantigens on their non-hematopoietic cells (62% vs. 100%; $P < 0.05$). GVL effects in [B6→B6] mice appeared to be almost equivalent to those in [B6→C3] mice given a 1-log lower T cell dose.

We further confirmed these observations in a different strain combination: BALB/c (Ba, H-2^d) and DBA/2 (Db, H-2^d) mice that

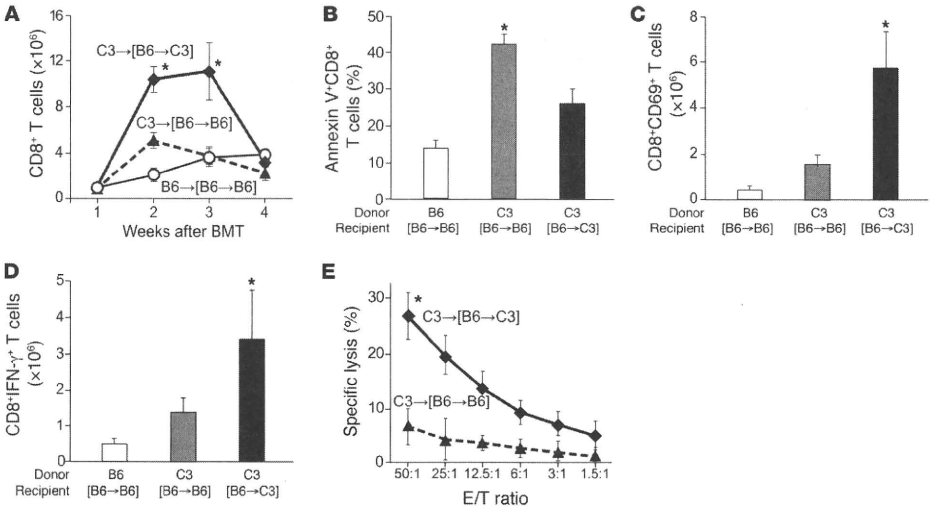

Figure 2

Alloantigen expression on host non-hematopoietic cells enhances the apoptosis and dysfunction of alloreactive T cells. [B6→C3] (diamonds and black bars) and [B6→B6] (triangles and gray bars) chimeras were transplanted as indicated in the legend for Figure 1. Syngeneic controls were [B6→B6] recipients of B6.Ly5.1 (CD45.1+) cells (open circles and white bars). (**A**) Numbers of donor CD8+ T cells in spleens. (**B**) Frequencies of annexin V+ donor CD8+ T cells. (**C**) Numbers of annexin V− donor CD69+CD8+ T cells. (**D**) Numbers of annexin V− IFN-γ–producing donor CD8+ T cells. (**E**) CTL activity against EL4. (**B–E**) Analysis was performed 14 days after BMT (n = 3–8/group). Representative data from 1 of the experiments are shown as the mean ± SD. *$P < 0.05$ compared with allogeneic controls.

differed at multiple mHAs from each other. [Db→Ba] and control [Db→Db] chimeras were lethally reirradiated and injected with 5×10^6 TCD BM cells alone or with 2×10^6 Ba T cells. Mortality (Figure 1D, $P = 0.08$) and morbidity from GVHD (Figure 1E, $P < 0.05$) were higher in [Db→Db] mice than in [Db→Ba] mice. When cells were transplanted together with 2,000 Db-derived P815 cells, leukemia mortality was significantly lower in [Db→Ba] mice than in [Db→Db] mice (10% vs. 60%; $P < 0.05$) (Figure 1F).

Similar results were obtained when [Ba→Db] and control [Ba→Ba] chimeras were transplanted with 5×10^6 TCD BM cells with or without 2×10^6 Db T cells. In [Ba→Db] recipients, in which non-hematopoietic cells do not express alloantigens, mortality (Figure 1G, $P = 0.08$) and morbidity of GVHD (Figure 1H, $P < 0.05$) were lower, but GVL effects against Ba-derived A20 lymphoma cells were significantly more potent as compared with [Ba→Ba] controls (leukemia mortality: 30% vs. 100%; $P < 0.05$) (Figure 1I). Taken together, these results demonstrate that GVHD is decreased but GVL activity is enhanced in the absence of alloantigen expression on non-hematopoietic cells.

Alloantigen expression on non-hematopoietic cells enhances apoptosis and dysfunction of alloreactive T cells. GVHD and GVL in the C3 and B6 strain combination is dependent on donor CD8+ T cells (12, 14). To elucidate the mechanisms responsible for the enhancement of the GVL effect in [B6→C3] chimeric mice, which lack alloantigen expression on non-hematopoietic cells, the kinetics of donor CD8+ T cell expansion and activation were evaluated after BMT. Expansion of donor CD8+ T cells identified as CD5.1+CD8+ cells peaked on day +14 in the spleens of allogeneic [B6→B6] recipients and decreased thereafter (Figure 2A), as previously shown in this model (15). CD8 expansion was significantly greater in [B6→C3] mice than in [B6→B6] mice on days +14 and +21. We next assessed donor T cell apoptosis as a determinant of the kinetics of T cell expansion. Frequencies of annexin V+ apoptotic donor CD8+ T cells were significantly greater in the spleen of [B6→B6] mice as compared with that of [B6→C3] mice on day +14 (Figure 2B). Notably, surviving donor CD8+ T cells were significantly less activated in [B6→B6] mice than in [B6→C3] mice when evaluated based on the expression of CD69 (Figure 2C) and intracellular IFN-γ (Figure 2D) on annexin V− donor CD8+ T cells. We next evaluated CTL activity in donor T cells isolated from the spleen on day +14 after BMT. CTL activity against EL4 targets was significantly reduced in the splenocytes of [B6→B6] mice as compared with [B6→C3] mice (Figure 2E). These results suggest that alloantigen expression on non-hematopoietic cells induces apoptosis and dysfunction of alloreactive T cells.

Absence of alloantigen expression on host non-hematopoietic cells restores GVL effects. Self-recognition in the periphery facilitates the reactivity of mature T cells to foreign antigens (16). Therefore, it is possible that the expression of syngeneic MHC molecules and not the absence of alloantigens on non-hematopoietic cells may be responsible for the enhancement of the GVL effect in [B6→C3] chimeras. This possibility was tested in B6-background $\beta_2m^{-/-}$ mice. [B6→$\beta_2m^{-/-}$] chimeras lacking functional MHC class I molecules on non-hematopoietic cells did not develop GVHD after transplantation with CD8+ T cells from C3 donors, as shown previously (17) (Figure 3A). In these mice, however, leukemia mortality was significantly delayed even in the absence of GVHD as compared with [B6→B6] recipients (Figure 3B, $P < 0.05$). The expansion and CTL activity of donor CD8+ T cells was significantly greater in [B6→$\beta_2m^{-/-}$] recipients than in [B6→B6] recipients (Figure 3, C and D).

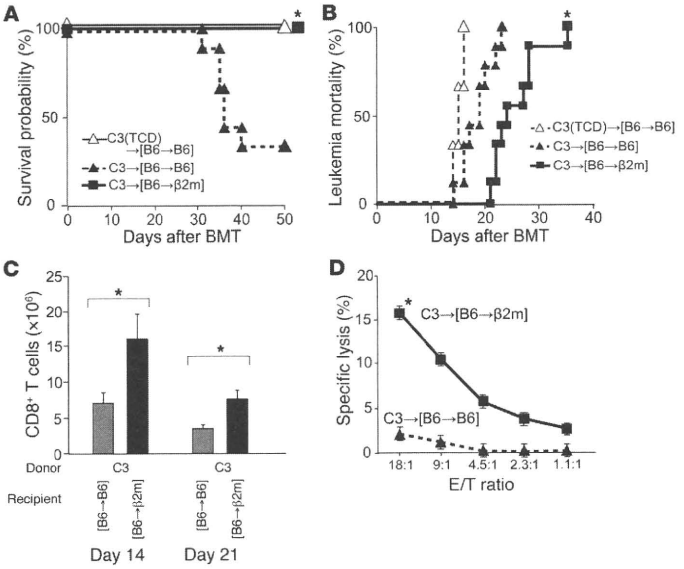

Figure 3
Absence of alloantigen expression on host nonhematopoietic cells restores GVL effects. [B6→B6] (triangles) and [B6→β2m$^{-/-}$] (squares) mice were reirradiated and injected with 5 × 10^6 TCD BM cells alone (open symbols) or with 1 × 10^6 CD8$^+$ T cells from C3 donors (filled symbols). (**A**) Survival after BMT. (**B**) Leukemia mortality in chimeras injected with EL4 cells (n = 6–9/group). Data from a representative experiment of 2 similar experiments are shown. Mean ± SEM numbers of donor CD8$^+$ T cells in spleens (n = 3–6/group) (**C**) and CTL activity against EL4 (**D**). *P < 0.05 compared with allogeneic controls.

These results confirm that alloantigen expression on host epithelium induces apoptosis and dysfunction of alloreactive T cells, which results in impaired GVL effects.

Alloantigen expression on host non-hematopoietic cells stimulates programmed death-1 and its ligand pathway. Programmed death-1 (PD-1) is a negative regulator of activated T cells and regulates T cell exhaustion during chronic infections (18–20). PD-1 interacts with at least 2 ligands: PD ligand-1 (PD-L1) and PD-L2 (21). In particular, the PD-1/PD-L1 pathway has been proposed as one of the most important mechanisms of T cell exhaustion and tolerance induction against infectious agents and tumors (19, 22–25). We therefore hypothesized that the PD-1/PD-L1 pathway plays a role in the loss of GVL effects in [B6→B6] mice. To test this hypothesis, we examined PD-1 expression on donor CD8$^+$ T cells in lymph nodes on day +14 and +21 after BMT. It was significantly upregulated in allogeneic [B6→B6] recipients as compared with syngeneic controls but was low in [B6→C3] mice (Figure 4, A and B). We also investigated the expression of another inhibitory receptor, CTLA-4, on donor CD8$^+$ T cells. Although the expression of cytoplasmic CTLA-4 was slightly upregulated in allogeneic animals as compared with syngeneic animals, its level did not differ between [B6→B6] and [B6→C3] mice (5.5% ± 1.0% vs. 4.5% ± 0.2%, respectively; P = 0.50).

We next examined PD-L1 expression in the liver by real-time PCR after BMT. PD-L1 expression was markedly upregulated in the liver of allogeneic controls as compared with syngeneic controls (Figure 4C). In allogeneic [B6→C3] mice, it was slightly upregulated on day +14 but not on day +21. Immunohistochemical analysis confirmed upregulated expression of PD-L1 in the liver of [B6→B6] mice, as previously reported (Figure 4D) (21, 26). These results showed that alloantigen expression on GVHD target epithelium is associated with upregulation of the PD-1/PD-L1 interactions between donor T cells and GVHD target tissue.

Blockade of the interaction between PD-1 and PD-L1 enhances GVL activity. We next examined whether blocking the PD-1/PD-L1 pathway could enhance GVL activity. [B6→C3] and [B6→B6] chimeras were reirradiated and injected with TCD BM cells and CD8$^+$ T cells from C3 donors. Mice were i.p. injected with 500 μg of anti–PD-L1 mAb on day 0 and then with 200 μg on days +3, +6, +9, +12, +15, and +18 after BMT. In [B6→B6] recipients, injection of anti–PD-L1 mAbs significantly restored T cell functions on day +14, as assessed by CD69 expression (Figure 5A), IFN-γ production (Figure 5B), and CTL activity (Figure 5C). In [B6→C3] mice, it marginally upregulated CD69 expression, IFN-γ production, and CTL activity, although differences were not statistically significant (Figure 5, A, B, and D). As a consequence, anti–PD-L1 mAb administration significantly increased the severity of GVHD in [B6→B6] mice (Figure 5E) but not in [B6→C3] mice (Figure 5F). PD-L1 blockade also significantly augmented GVL activity in [B6→B6] recipients injected with EL4 cells on day 0 (Figure 5G, P < 0.05). It also delayed leukemia death in [B6→C3] mice, although the difference was not statistically significant (Figure 5H, P = 0.38). In controls, PD-L1 blockade did not affect leukemia mortality in TCD-BMT recipients (Figure 5H) or [B6→B6] recipients of syngeneic B6 CD8$^+$ T cells (data not shown).

Discussion

Alloantigens are expressed in three major sites in HSCT recipients: APCs, GVHD target epithelium, and leukemia cells. Alloantigen expression on APCs is essential for the induction of GVHD (6), and an optimal GVL response occurs when alloantigens are expressed on both host APCs and tumor cells (7). Alloantigen expression on the epithelium is also critical for the induction of GVHD across mHA disparities (10), but GVHD can occur in the absence of alloantigen expression on epithelium in MHC-mismatched BMT (9). In this study, we addressed the effect of alloantigen expression on target epithelium in GVL using chimeric mouse models of GVHD and GVL across mHA disparities. Our models mimic clinical BMT in patients not in remission, since most of the mice relapsed after allogeneic BMT. This high tumor burden enabled us to compare the magnitude of GVL activity in our models, and we made sur-

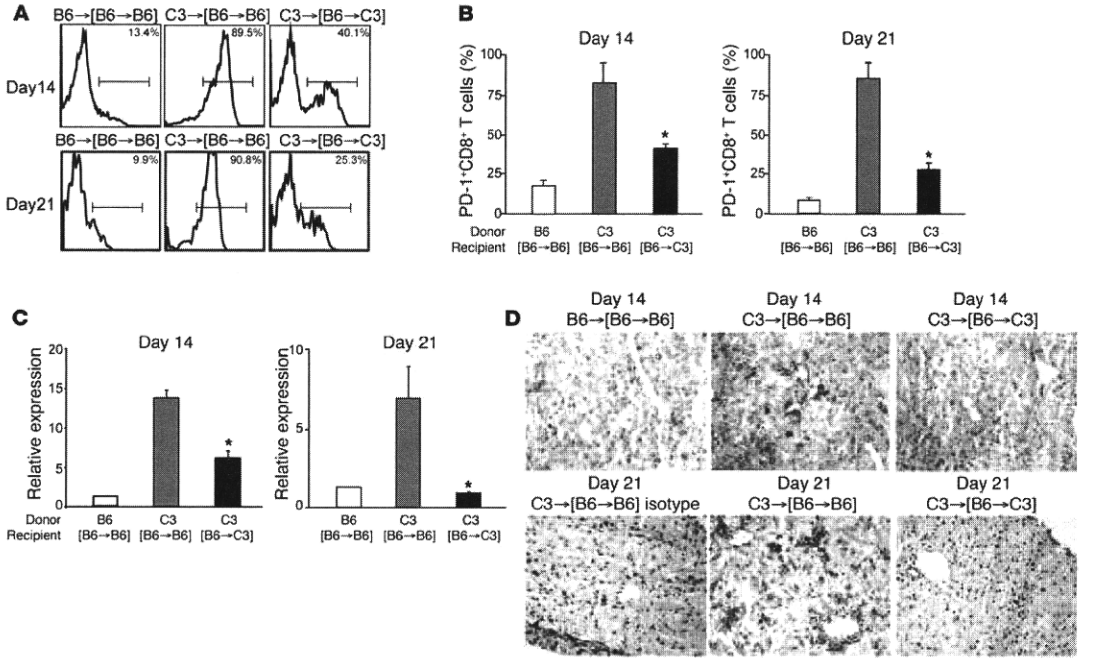

Figure 4

Alloantigen expression on host non-hematopoietic cells stimulates PD-1 and its ligand pathway. [B6→B6] and [B6→C3] chimeras were transplanted as indicated in the legend for Figure 1 ($n = 4–8$). (**A**) Representative histogram of PD-1 expression among donor CD8$^+$ T cells on day +14 and +21 in syngeneic (left), allogeneic [B6→B6] (middle), and [B6→C3] (right) recipients. (**B**) Frequencies of PD-1$^+$ CD8$^+$ T cells (mean ± SD). (**C**) Relative expressions of *Pdl1* mRNA on day +14 and +21 in the livers of allogeneic [B6→B6] (gray bars) and allogeneic [B6→C3] mice (black bars). Data represent the mean (± SD) of *n*-fold difference in the amount of *Pdl1* gene expression relative to that in syngeneic mice. (**D**) PD-L1 expression in the liver on day +14 (top row) and +21 (bottom row) from syngeneic (upper left) and allogeneic [B6→B6] (middle) and [B6→C3] (right) recipients. Isotype control of allogeneic [B6→B6] (lower left) is shown. Original magnification, ×200. *$P < 0.05$ compared with allogeneic controls.

prising observations that alloantigen expression on non-hematopoietic cells inhibited GVL effects but enhanced GVHD. This observation challenges the current paradigm that GVL activity is strongly correlated with the severity of GVHD (1, 2, 27).

We found that alloantigen expression on non-hematopoietic cells induced donor T cell apoptosis and led to a contraction in the size of an alloreactive donor CD8$^+$T cell pool early after BMT. The remainder of the donor T cells were alive, but their ability to produce cytokines and cytotoxicity were impaired. This defect is similar to T cell exhaustion, which is a principal reason for the inability of the host to eliminate the persisting pathogen in chronic infections (18, 28). CD8$^+$ T cell proliferation and differentiation into cytolytic effectors on an encounter with antigens are variable and change as a consequence of the antigen load (29). As the magnitude of the viral load increases, virus-specific T cells become more functionally impaired. During persistent infection, a high antigen load drives a significant number of virus-specific T cells into activation-induced apoptosis, and the remaining virus-specific T cells remain alive but in a dysfunctional state of cytotoxicity (18, 30–33). In tumor models, antigen quantity determines the behavior of the CD8$^+$ effector cells, including their effector function and sensitivity to apoptosis (34–36). In patients with a larger tumor burden, CD8$^+$ T cells were found to undergo apoptosis (37). Thus, a higher alloantigen load in allogeneic controls as compared with chimeras, in which alloantigen expression is limited to hematopoietic cells and tumor cells, may induce apoptosis and the dysfunction of alloreactive T cells, which leads to the inability of the host to eliminate leukemia.

Our results are consistent with seminal observations by Meunier, Fontaine, and colleagues, who showed that the adoptive transfer of immunodominant mHA ($B6^{dom1}$)-specific T cells eradicates $B6^{dom1}$-expressing leukemia more efficiently in mice lacking $B6^{dom1}$ expression than in mice expressing $B6^{dom1}$ (38). This was because the widespread expression of $B6^{dom1}$ caused activation-induced apoptosis and dysfunction of donor T cells in mice expressing $B6^{dom1}$ (38, 39). These findings along with our results indicate that allogeneic cellular therapy targeting mHAs exclusively expressed on APCs and tumor cells can induce a potent GVL effect while inducing less-severe GVHD than immunotherapy via targeting of ubiquitously expressed mHAs (40).

The PD-1/PD-L1 pathway is critically involved in T cell exhaustion and tolerance induction in infection and tumor immunology (18–20, 23–25, 41). It is also required for protection against chronic rejection of cardiac allograft, and induction of peripheral dele-

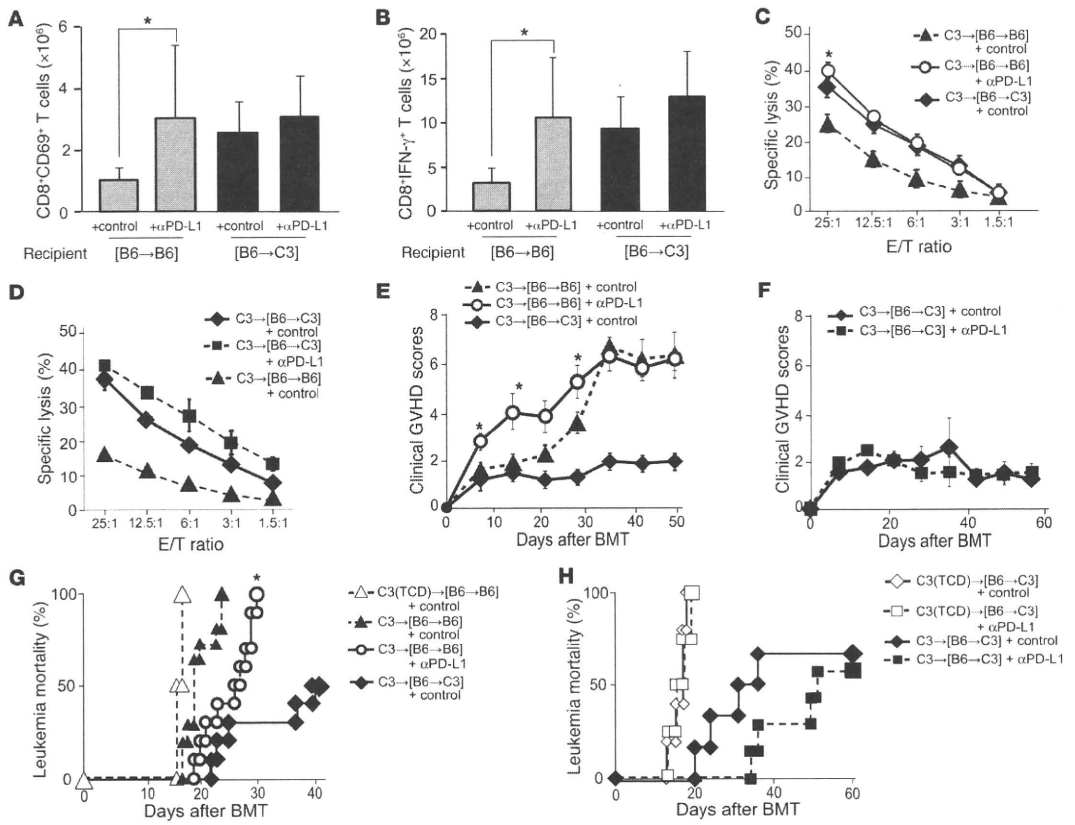

Figure 5

Blockade of the interaction between PD-1 and PD-L1 enhances GVL activity. [B6→C3] and [B6→B6] chimeras were reirradiated and injected with 5 × 10^6 TCD BM cells alone or with 1 × 10^6 $CD8^+$ T cells from C3 donors. Mice were i.p. injected with 500 μg of anti PD-L1 mAbs or controls on day 0 and then 200 μg thereafter on days +3, +6, +9, +12, +15, and +18. Splenocytes were harvested on day +14 to determine the number of $CD8^+CD69^+$ T cells (**A**) and IFN-γ–producing $CD8^+$ T cells (**B**) and CTL activity against EL4 targets (**C** and **D**). Results from a representative experiment of 2 similar experiments (means ± SD, n = 7–8/group). Mean clinical GVHD scores (±SEM) (**E** and **F**) after BMT are shown (n = 5–7/group). (**G** and **H**) Leukemia mortality after BMT in [B6→B6] and [B6→C3] chimeras injected with EL4 cells on day 0 (n = 4–11/group). Data from two similar experiments were combined. αPD-L1, anti–PD-L1 mAbs. *P < 0.05 compared with the corresponding controls.

tional tolerance of alloreactive, anti-donor $CD8^+$ T cells to achieve successful engraftment in BMT (42, 43). In this study, we found that PD-1 expression was upregulated in donor T cells and PD-L1 expression was upregulated in GVHD target organs. The expression of PD-1/PD-L1 was markedly reduced in chimeras lacking alloantigen expression on non-hematopoietic cells. PD-1 and PD-L1 expression is induced upon cell activation and inflammation in GVHD (44); therefore, the absence of alloantigen expression on GVHD target epithelium reduced GVHD in chimeric mice, which resulted in insufficient stimulation of the PD-1/PD-L1 interaction. Target tissue expression of PD-L1 is also critical for the induction of T cell exhaustion or tolerance in chronic viral infection, autoimmune diabetes, and cardiac allografting (19, 42, 45).

Both PD-1 and PD-L1 were markedly upregulated in [B6→B6] mice, but they were also modestly upregulated in [B6→C3] mice. Blockade of PD-1/PD-L1 interactions significantly restored T cell effector functions in [B6→B6] mice but modestly restored them in [B6→C3] mice as well. The relevance of these observations is shown by the PD-1/PD-L1 blockade studies. These data showed that the PD-1/PD-L1 pathway is particularly germane to [B6→B6] mice with widespread expression of alloantigens but also applies, at least in part, to [B6→C3] mice, wherein alloantigen expression is only on APCs. While there is likely to be a role for this pathway in the absence of epithelial alloantigen expression, the full negative impact of this pathway on GVL is only seen when alloantigen expression is present on non-hematopoietic tissues.

Of note, the improvement in GVL by the PD-1/PD-L1 blockade was partial, as has been shown in chronic viral infection (46–48). This may be due to the presence of multiple negative regulatory pathways that contribute to T cell exhaustion, including CTLA-4, IL-10, LAG-3, CD160, and 2B4 (20, 47, 49). In addition, the population of exhausted T cells is heterogeneous, and this interven-

tion is effective only for PD-1^{lo} and not PD-1^{hi}, which are subsets of exhausted T cells (50). Many of these inhibitory receptors are either coexpressed by the same exhausted T cells or differentially expressed on different subsets of exhausted cells. As the severity of the infection increases, the number of different inhibitors expressed per cell increases (47). A second inhibitory receptor, CTLA-4, can be overexpressed by exhausted CD4$^+$ T cells in chronic viral infection, but it appears to have a minimal role on exhausted CD8$^+$ T cells (19, 51). Although CTLA-4 was only slightly upregulated on CD8$^+$ T cells in contrast to the marked upregulation of PD-1 in our CD8-dependent model of MHC-matched BMT, the precise inhibitory receptors of therapeutic interest may differ between CD4$^+$-dependent and CD8$^+$-dependent GVHD/GVL. Another key negative regulatory pathway is mediated by Foxp3$^+$ Tregs. However, enhancement of GVL is not due to effects of the PD-1/PD-L1 blockade on Tregs, because blockade of PD-1/PD-L1 interactions enhances the expansion and function of Tregs (52). The hierarchy of these pathways in regulating GVL will need to be studied in the future based on better understanding of the delineation of T cell subsets and models (53). However, our results suggest the detrimental effect of GVHD-induced immunosuppression on GVL responses, regardless of which inhibitory pathway might be dominant clinically.

In addition, the administration of anti-PD-L1 mAb also exacerbated acute GVHD, as has been shown in a previous study (54). Therefore, the beneficial effects of the PD-1/PD-L1 blockade may be offset by the exacerbation of GVHD. Effects of the inhibitory receptor blockade might depend on the magnitude or stage of donor T cell activation and the severity of GVHD; therefore, the timing and duration of the targeting may be important.

In clinical HSCT, alloantigens continue to be presented on MHC class I in non-hematopoietic cells throughout the lifetime of the transplant recipients. However, a substantial number of patients eventually develop tolerance after resolution of GVHD and often experience leukemia relapse. Although activation-induced apoptosis of alloreactive T cells has been proposed as an explanation of this paradox (55), studies monitoring GVHD-specific T cell clones indicate that host-reactive T cells are continuously present after allogeneic HSCT (56–58). Our results provide a logical explanation for this paradox. However, the process of exhaustion is unlikely to occur in patients not developing GVHD, because induction of T cell exhaustion requires antigen-specific activation of T cells and subsequent differentiation into effector T cells. In these patients, tolerance could be induced by other mechanisms, such as functional central and peripheral tolerance mechanisms. It is well known that GVL is not apparent in patients with high leukemia burden. Although leukemia cells used in the current study do not express PD-L1 (22, 59), leukemia cells expressing PD-L1 may also directly limit the GVL response in patients with high leukemia burden (22, 24, 25). However, such insights from animal models must be extrapolated with caution to clinical studies involving humans.

It has been assumed that T cell exhaustion is antigen specific in chronic viral infection. Bystander lysis of T cells has also been reported in the course of viral infections (60), but is of minimal significance because of its limited magnitude and because normal thymic function can replenish the peripheral T cell pool. In contrast, in GVHD, T cell exhaustion occurs after initial T cell activation and the subsequent development of GVHD. GVHD induces bystander apoptosis of non-host-reactive T cells. In addition, GVHD-mediated injury of the thymus and the secondary lymphoid organs inhibits full replenishment of the peripheral T cell pool (55). Thus, establishment of full immune competence probably requires the additional process of T cell reconstitution following T cell exhaustion.

In conclusion, our results indicated the significance of alloantigen expression on non-hematopoietic cells in GVL. Alloantigen expression on non-hematopoietic cells induces the apoptosis of donor T cells and the dysfunction of cytotoxic effector function, which leads to a reduction in GVL activity. T cell dysfunction was partially restored by blocking PD-1/PD-L1 interactions, which suggests that the therapeutic "tuning" of T cell responses via modulation of negative regulatory pathways represents a novel strategy for enhancing GVL. Our results in combination with those of previous studies (6, 7, 9, 10, 38, 39) provide a complete picture of the effect of alloantigen expression on host APCs, GVHD target epithelium, and tumor cells in allogeneic HSCT; alloantigen expression on host non-hematopoietic cells augments GVHD but suppresses GVL effects. This concept may provide an important framework for understanding the pathophysiology of GVHD and allow for the separation of GVHD and GVL.

Methods

Mice. Female C57BL/6 (B6, H-2^b, CD45.2$^+$), BALB/c (Ba, H-2^d), and DBA/2 (Db, H-2^d) mice were purchased from Charles River Japan. B6.Ly5.1 (H-2^b, CD45.1$^+$) and C3H.Sw (C3, H-2^b) mice were purchased from The Jackson Laboratory. B6-background β_2m-deficient mice ($\beta_2m^{-/-}$: B6.129-β_2-m^{tm1Jae}N12) were purchased from Taconic. The age of mice used ranged from 8 to 12 weeks. Mice were maintained in specific pathogen-free conditions and received normal chaw and hyperchlorinated drinking water for the first 3 weeks after BMT. All experiments involving animals were performed according to a protocol approved by the Institutional Animal Care and Research Advisory Committee of Okayama University and Kyushu University.

Generation of bone marrow chimera and induction of GVHD and GVL. Total body irradiation (TBI: X-ray) was split into 2 doses separated by 4 hours to minimize gastrointestinal toxicity. B6 and C3 mice received 10 Gy TBI, whereas Ba and Db mice received 8.5 Gy TBI. To create BM chimeras, lethally irradiated mice were intravenously injected with 5×10^6 TCD BM cells from donors. TCD was performed using anti-CD90 microbeads and AutoMACS (Miltenyi Biotec). Four months later, the chimeric mice were reirradiated and injected with 5×10^6 TCD BM cells plus various doses of CD8$^+$ T cells or 2×10^6 T cells. T cells and CD8$^+$ T cells were negatively isolated from splenocytes by using a T cell isolation kit and a CD8$^+$ T cell isolation kit (Miltenyi Biotec), respectively, and the AutoMACS. In the GVL experiments, EL4 (H-2^b) derived from a B6 mouse, P815 (H-2^d) derived from a Db mouse, and A20 (H-2^d) derived from a Ba mouse were intravenously injected into BMT recipients on day 0 of BMT. Anti-PD-L1 mAbs were purified from the hybridoma supernatant of clone MIH5 (61), which was a gift from Miyuki Azuma of Tokyo Medical and Dental University, Tokyo, Japan, and i.p. injected at a dose of 500 μg/mouse on day 0, followed by 200 μg/mouse on days +3, +6, +9, +12, +15, and +18 after BMT.

Assessment of GVHD and GVL effects. Survival after BMT was monitored daily, and the degree of clinical GVHD was assessed weekly by using a scoring system that sums changes in 5 clinical parameters: weight loss, posture, activity, fur texture, and skin integrity (maximum index, 10) as described previously (13). The cause of each death after BMT was determined by post mortem examination, and was either GVHD or tumor. The most striking leukemia-specific abnormality induced by EL4, P815, and A20 was macroscopic tumor nodules, marked hepatosplenomegaly, and lower limb paralysis (62). Leukemia death induced by EL4, P815, and A20 was therefore defined by the occurrence of hepatosplenomegaly, macroscopic tumor nodules in the liver

and/or spleen, or hind leg paralysis. GVHD death was defined as the absence of leukemia and by the presence of clinical signs of GVHD, assessed by using a clinical scoring system. Animals surviving beyond the observation period of BMT were sacrificed, and the spleen and liver were harvested for histological evaluation to determine leukemia-free survival.

Flow cytometric analysis. The mAbs used were FITC-, PE-, PerCP-, Cy5.5-, or APC-conjugated anti-mouse CD5.1, CD8, CD45.1, CD45.2, CD69, and PD-1 (BD Biosciences). Cells positive for 7-amino-actinomycin D (BD Biosciences) were excluded from the analysis. For the analysis of donor T cell apoptosis, the cells were stained with Annexin V (MBL). For intracellular IFN-γ staining, the splenocytes were incubated for 4 hours with leukocyte activation cocktail and BD GolgiPlug (BD Biosciences) at 37°C. Then, the cells underwent permeabilization with a BD Cytofix/Cytoperm solution (BD Biosciences) and were stained with FITC-conjugated anti-IFN-γ mAbs (BD Biosciences). For intracellular CTLA-4 staining, cells were stained with PE-conjugated anti-CTLA-4 mAbs (eBioscience). At least 5,000 live events were acquired for the analysis using a FACSCalibur flow cytometer (BD Biosciences).

CTL assay. Splenocytes were removed from chimeric recipients 14 days after BMT, and the mononuclear cells were then separated by density gradient centrifugation. The percentage of $CD8^+$ cells in this fraction was determined by flow cytometry, and counts were normalized for $CD8^+$ cell numbers. Tumor targets, 2×10^6 P815 or EL4, were labeled with 100 μCi of ^{51}Cr sodium salt (Amersham Biosciences) for 2 hours. After washing 3 times, the labeled targets were resuspended in 10% FCS in RPMI and plated at 10^4 cells per well in U-bottom plates (Corning-Costar Corp.). Allogeneic splenocyte preparations, as described above, were added to quadruplicate wells at varying effector-to-target ratios and incubated for 4 hours. Maximal and background release were determined by adding 1% SDS and media alone to the targets, respectively. ^{51}Cr activity in the supernatants collected 4 hours later was determined using a Wallac 1470 WIZARD Gamma Counter (Wallac Oy), and lysis was expressed as a percentage of maximum: percentage of specific lysis = 100 (sample count − background count/maximum count − background count).

Quantitative real-time PCR. Total RNA was isolated from the frozen liver using ISOGEN (Nippon Gene). cDNA was synthesized from 150 μg RNA using a QuantiTect Reverse Transcription Kit (QIAGEN). *Pdl1* mRNA levels were quantified by real-time PCR using the 7500 Real-Time PCR System (Applied Biosystems). TaqMan Universal PCR MasterMix, primers, and the fluorescent TaqMan probe specific for murine PD-L1 (Mm00452054-m1) and a house keeping gene, mGAPDH (Mm99999915-g1), were purchased from Applied Biosystems. The standard was obtained using RNA extracted from syngeneic controls.

Immunohistochemistry. For immunohistochemical analysis, isolated livers were frozen in Tissue-Tek (Sakura Finetek), and 5-μm cryostat sections were prepared. Slides were fixed in 100% acetone and air dried. Endogenous peroxidase activity was blocked with peroxidase blocking reagent (Dako). The sections were incubated with purified rat anti-mouse PD-L1 mAb (clone MIH5; eBiosciences). The primary Abs were detected using the Histofine Simple Stain Mouse MAX PO (Rat) kit and DAB solution (Nichirei). The images were captured using an Olympus BH2 microscope with a Nikon DS-5M color digital camera (Nikon), controlled by Nikon ATC-2U software version 1.5. An Olympus ×10/20 ocular lens and a ×20/0.46 NA objective lens were used. Images were cropped using Adobe Photoshop (Adobe Systems) and were composed using Adobe Illustrator.

Statistics. We used the Kaplan-Meier product-limit method to obtain survival probability and the log-rank test to compare survival curves. The Mann-Whitney *U* test was used to analyze the clinical scores. A *P* value less than 0.05 was considered statistically significant.

Acknowledgments

We thank Miyuki Azuma of Tokyo Medical and Dental University for providing hybridoma MIH5-producing anti-PD-L1 mAbs. This study was supported by grant 21390295 from the Ministry of Education, Culture, Sports, Science, and Technology (Tokyo, Japan) (to T. Teshima), Health and Labor Science Research Grants (Tokyo, Japan) (to T. Teshima), and a grant from the Foundation for Promotion of Cancer Research (Tokyo, Japan) (to T. Teshima).

Received for publication March 11, 2009, and accepted in revised form April 7, 2010.

Address correspondence to: Takanori Teshima, Center for Cellular and Molecular Medicine, Kyushu University Hospital, 3-1-1 Maidashi, Higashi-ku, Fukuoka 812-8582, Japan. Phone: 81.92.642.5947; Fax: 81.92.642.5951; E-mail: tteshima@cancer.med.kyushu-u.ac.jp.

1. Weiden P, et al. Antileukemic effect of graft-versus-host disease in human recipients of allogeneic-marrow grafts. *N Engl J Med.* 1979;300(19):1068–1073.
2. Weiden PL, Sullivan KM, Flournoy N, Storb R, Thomas ED. Antileukemic effect of chronic graft-versus-host disease: contribution to improved survival after allogeneic marrow transplantation. *N Engl J Med.* 1981;304(25):1529–1533.
3. Korngold R, Sprent J. Lethal graft-versus-host disease after bone marrow transplantation across minor histocompatibility barriers in mice. Prevention by removing mature T-cells from marrow. *J Exp Med.* 1978;148(6):1687–1698.
4. Apperley JF, Jones L, Hale G, Goldman JM. Bone marrow transplantation for chronic myeloid leukemia: T-cell depletion with Campath-1 reduces the incidence of acute graft-versus-host disease but may increase the risk of leukemia relapse. *Bone Marrow Transplant.* 1986;1(1):53–66.
5. Atkinson K, et al. Risk factors for chronic graft-versus-host disease after HLA-identical sibling bone marrow transplantation. *Blood.* 1990;75(12):2459–2464.
6. Shlomchik WD, et al. Prevention of graft versus host disease by inactivation of host antigen-presenting cells. *Science.* 1999;285(5426):412–415.
7. Reddy P, Maeda Y, Liu C, Krijanovski OI, Korngold R, Ferrara JL. A crucial role for antigen-presenting cells and alloantigen expression in graft-versus-leukemia responses. *Nat Med.* 2005;11(11):1244–1249.
8. Bleakley M, Riddell SR. Molecules and mechanisms of the graft-versus-leukaemia effect. *Nat Rev Cancer.* 2004;4(5):371–380.
9. Teshima T, et al. Acute graft-versus-host disease does not require alloantigen expression on host epithelium. *Nat Med.* 2002;8(6):575–581.
10. Jones SC, Murphy GF, Friedman TM, Korngold R. Importance of minor histocompatibility antigen expression by nonhematopoietic tissues in a CD4+ T cell-mediated graft-versus-host disease model. *J Clin Invest.* 2003;112(12):1880–1886.
11. Ruggeri L, et al. Effectiveness of donor natural killer cell alloreactivity in mismatched hematopoietic transplants. *Science.* 2002;295(5562):2097–2100.
12. Matte CC, et al. Donor APCs are required for maximal GVHD but not for GVL. *Nat Med.* 2004;10(9):987–992.
13. Cooke KR, et al. An experimental model of idiopathic pneumonia syndrome after bone marrow transplantation. I. The roles of minor H antigens and endotoxin. *Blood.* 1996;88(8):3230–3239.
14. Korngold R, Sprent J. Features of T cells causing H-2-restricted lethal graft-vs.-host disease across minor histocompatibility barriers. *J Exp Med.* 1982;155(3):872–883.
15. Zhang Y, Joe G, Hexner E, Zhu J, Emerson SG. Alloreactive memory T cells are responsible for the persistence of graft-versus-host disease. *J Immunol.* 2005;174(5):3051–3058.
16. Stefanova I, Dorfman JR, Germain RN. Self-recognition promotes the foreign antigen sensitivity of naive T lymphocytes. *Nature.* 2002;420(6914):429–434.
17. Zhang Y, Louboutin JP, Zhu J, Rivera AJ, Emerson SG. Preterminal host dendritic cells in irradiated mice prime CD8+ T cell-mediated acute graft-versus-host disease. *J Clin Invest.* 2002;109(10):1335–1344.
18. Zajac AJ, et al. Viral immune evasion due to persistence of activated T cells without effector function. *J Exp Med.* 1998;188(12):2205–2213.
19. Barber DL, et al. Restoring function in exhausted CD8 T cells during chronic viral infection. *Nature.* 2006;439(7077):682–687.
20. Shin H, Wherry EJ. CD8 T cell dysfunction during chronic viral infection. *Curr Opin Immunol.* 2007;19(4):408–415.
21. Keir ME, Butte MJ, Freeman GJ, Sharpe AH. PD-1 and its ligands in tolerance and immunity. *Annu Rev Immunol.* 2008;26:677–704.
22. Dong H, et al. Tumor-associated B7-H1 promotes T-cell apoptosis: a potential mechanism of immune evasion. *Nat Med.* 2002;8(8):793–800.
23. Ahmadzadeh M, et al. Tumor antigen-specific CD8

T cells infiltrating the tumor express high levels of PD-1 and are functionally impaired. *Blood.* 2009; 114(8):1537–1544.
24. Zhang L, Gajewski TF, Kline J. PD-1/PD-L1 interactions inhibit anti-tumor immune responses in a murine acute myeloid leukemia model. *Blood.* 2009; 114(8):1545–1552.
25. Mumprecht S, Schurch C, Schwaller J, Solenthaler M, Ochsenbein AF. PD-1 signaling on chronic myeloid leukemia-specific T cells results in T cell exhaustion and disease progression. *Blood.* 2009; 114(8):1528–1536.
26. Iwai Y, Terawaki S, Ikegawa M, Okazaki T, Honjo T. PD-1 inhibits antiviral immunity at the effector phase in the liver. *J Exp Med.* 2003;198(1):39–50.
27. Horowitz MM, et al. Graft-versus-leukemia reactions after bone marrow transplantation. *Blood.* 1990;75(3):555–562.
28. Gallimore A, et al. Induction and exhaustion of lymphocytic choriomeningitis virus-specific cytotoxic T lymphocytes visualized using soluble tetrameric major histocompatibility complex class I-peptide complexes. *J Exp Med.* 1998;187(9):1383–1393.
29. Welsh RM. Assessing CD8 T cell number and dysfunction in the presence of antigen. *J Exp Med.* 2001; 193(5):F19–F22.
30. Moskophidis D, Lechner F, Pircher H, Zinkernagel RM. Virus persistence in acutely infected immunocompetent mice by exhaustion of antiviral cytotoxic effector T cells. *Nature.* 1993;362(6422):758–761.
31. Appay V, et al. HIV-specific CD8(+) T cells produce antiviral cytokines but are impaired in cytolytic function. *J Exp Med.* 2000;192(1):63–75.
32. Xiong Y, et al. Simian immunodeficiency virus (SIV) infection of a rhesus macaque induces SIV-specific CD8(+) T cells with a defect in effector function that is reversible on extended interleukin-2 incubation. *J Virol.* 2001;75(6):3028–3033.
33. Pantaleo G, Harari A. Functional signatures in antiviral T-cell immunity for monitoring virus-associated diseases. *Nat Rev Immunol.* 2006;6(5):417–423.
34. Tham EL, Mescher MF. Signaling alterations in activation-induced nonresponsive CD8 T cells. *J Immunol.* 2001;167(4):2040–2048.
35. Tham EL, Shrikant P, Mescher MF. Activation-induced nonresponsiveness: a Th-dependent regulatory checkpoint in the CTL response. *J Immunol.* 2002;168(3):1190–1197.
36. Boissonnas A, et al. Antigen distribution drives programmed antitumor CD8 cell migration and determines its efficiency. *J Immunol.* 2004;173(1):222–229.
37. Saito T, Dworacki G, Gooding W, Lotze MT, Whiteside TL. Spontaneous apoptosis of CD8+ T lymphocytes in peripheral blood of patients with advanced melanoma. *Clin Cancer Res.* 2000;6(4):1351–1364.
38. Fontaine P, Roy-Proulx G, Knafo L, Baron C, Roy DC, Perreault C. Adoptive transfer of minor histocompatibility antigen-specific T lymphocytes eradicates leukemia cells without causing graft-versus-host disease. *Nat Med.* 2001;7(7):789–794.
39. Meunier MC, Roy-Proulx G, Labrecque N, Perreault C. Tissue distribution of target antigen has a decisive influence on the outcome of adoptive cancer immunotherapy. *Blood.* 2003;101(2):766–770.
40. Dickinson AM, et al. In situ dissection of the graft-versus-host activities of cytotoxic T cells specific for minor histocompatibility antigens. *Nat Med.* 2002; 8(4):410–414.
41. Ding ZC, Blazar BR, Mellor AL, Munn DH, Zhou G. Chemotherapy rescues tumor-driven aberrant CD4+ T-cell differentiation and restores an activated polyfunctional helper phenotype. *Blood.* 2010; 115(12):2397–2406.
42. Tanaka K, et al. PDL1 is required for peripheral transplantation tolerance and protection from chronic allograft rejection. *J Immunol.* 2007; 179(8):5204–5210.
43. Haspot F, et al. Peripheral deletional tolerance of alloreactive CD8 but not CD4 T cells is dependent on the PD-1/PD-L1 pathway. *Blood.* 2008; 112(5):2149–2155.
44. Yamazaki T, et al. Expression of programmed death 1 ligands by murine T cells and APC. *J Immunol.* 2002;169(10):5538–5545.
45. Keir ME, et al. Tissue expression of PD-L1 mediates peripheral T cell tolerance. *J Exp Med.* 2006; 203(4):883–895.
46. Crawford A, Wherry EJ. The diversity of costimulatory and inhibitory receptor pathways and the regulation of antiviral T cell responses. *Curr Opin Immunol.* 2009;21(2):179–186.
47. Blackburn SD, et al. Coregulation of CD8+ T cell exhaustion by multiple inhibitory receptors during chronic viral infection. *Nat Immunol.* 2009; 10(1):29–37.
48. Petrovas C, et al. PD-1 is a regulator of virus-specific CD8+ T cell survival in HIV infection. *J Exp Med.* 2006;203(10):2281–2292.
49. Brooks DG, Trifilo MJ, Edelmann KH, Teyton L, McGavern DB, Oldstone MB. Interleukin-10 determines viral clearance or persistence in vivo. *Nat Med.* 2006;12(11):1301–1309.
50. Blackburn SD, Shin H, Freeman GJ, Wherry EJ. Selective expansion of a subset of exhausted CD8 T cells by alphaPD-L1 blockade. *Proc Natl Acad Sci U S A.* 2008;105(39):15016–15021.
51. Kaufmann DE, et al. Upregulation of CTLA-4 by HIV-specific CD4+ T cells correlates with disease progression and defines a reversible immune dysfunction. *Nat Immunol.* 2007;8(11):1246–1254.
52. Franceschini D, et al. PD-L1 negatively regulates CD4+CD25+Foxp3+ Tregs by limiting STAT-5 phosphorylation in patients chronically infected with HCV. *J Clin Invest.* 2009;119(3):551–564.
53. Socie G, Blazar BR. Acute graft-versus-host disease: from the bench to the bedside. *Blood.* 2009; 114(20):4327–4336.
54. Blazar BR, et al. Blockade of programmed death-1 engagement accelerates graft-versus-host disease lethality by an IFN-gamma-dependent mechanism. *J Immunol.* 2003;171(3):1272–1277.
55. Brochu S, Rioux-Masse B, Roy J, Roy DC, Perreault C. Massive activation-induced cell death of alloreactive T cells with apoptosis of bystander postthymic T cells prevents immune reconstitution in mice with graft-versus-host disease. *Blood.* 1999;94(2):390–400.
56. Dey B, et al. The fate of donor T-cell receptor transgenic T cells with known host antigen specificity in a graft-versus-host disease model. *Transplantation.* 1999;68(1):141–149.
57. Choi EY, et al. Real-time T-cell profiling identifies H60 as a major minor histocompatibility antigen in murine graft-versus-host disease. *Blood.* 2002; 100(13):4259–4265.
58. Michalek J, Collins RH, Hill BJ, Brenchley JM, Douek DC. Identification and monitoring of graft-versus-host specific T-cell clone in stem cell transplantation. *Lancet.* 2003;361(9364):1183–1185.
59. Hirano F, et al. Blockade of B7-H1 and PD-1 by monoclonal antibodies potentiates cancer therapeutic immunity. *Cancer Res.* 2005;65(3):1089–1096.
60. Ando K, et al. Perforin, Fas/Fas ligand, and TNF-alpha pathways as specific and bystander killing mechanisms of hepatitis C virus-specific human CTL. *J Immunol.* 1997;158(11):5283–5291.
61. Tsushima F, et al. Preferential contribution of B7-H1 to programmed death-1-mediated regulation of hapten-specific allergic inflammatory responses. *Eur J Immunol.* 2003;33(10):2773–2782.
62. Teshima T, et al. IL-11 separates graft-versus-leukemia effects from graft-versus-host disease after bone marrow transplantation. *J Clin Invest.* 1999;104(3):317–325.

THE JOURNAL OF IMMUNOLOGY

Altered Effector CD4$^+$ T Cell Function in IL-21R $^{-/-}$ CD4$^+$ T Cell-Mediated Graft-Versus-Host Disease

Iekuni Oh, Katsutoshi Ozaki, Akiko Meguro, Keiko Hatanaka, Masanori Kadowaki, Haruko Matsu, Raine Tatara, Kazuya Sato, Yoichiro Iwakura, Susumu Nakae, Katsuko Sudo, Takanori Teshima, Warren J. Leonard and Keiya Ozawa

J Immunol 2010;185;1920-1926; Prepublished online 23 June 2010;
doi:10.4049/jimmunol.0902217
http://www.jimmunol.org/content/185/3/1920

The Journal of Immunology is published twice each month by The American Association of Immunologists, Inc., 9650 Rockville Pike, Bethesda, MD 20814-3994.

Print ISSN: 0022-1767 Online ISSN: 1550-6606.

Altered Effector CD4$^+$ T Cell Function in IL-21R$^{-/-}$ CD4$^+$ T Cell-Mediated Graft-Versus-Host Disease

Iekuni Oh,* Katsutoshi Ozaki,* Akiko Meguro,* Keiko Hatanaka,* Masanori Kadowaki,† Haruko Matsu,* Raine Tatara,* Kazuya Sato,* Yoichiro Iwakura,‡ Susumu Nakae,§ Katsuko Sudo,¶ Takanori Teshima,† Warren J. Leonard,‖ and Keiya Ozawa*

We previously showed that transplantation with *IL-21R* gene-deficient splenocytes resulted in less severe graft-versus-host disease (GVHD) than was observed with wild type splenocytes. In this study, we sought to find mechanism(s) explaining this observation. Recipients of donor CD4$^+$ T cells lacking IL-21R exhibited diminished GVHD symptoms, with reduced inflammatory cell infiltration into the liver and intestine, leading to prolonged survival. After transplantation, CD4$^+$ T cell numbers in the spleen were reduced, and MLR and cytokine production by CD4$^+$ T cells were impaired. These results suggest that IL-21 might promote GVHD through enhanced production of effector CD4$^+$ T cells. Moreover, we found that CD25 depletion altered neither the impaired MLR in vitro nor the ameliorated GVHD symptoms in vivo. Thus, the attenuated GVHD might be caused by an impairment of effector T cell differentiation itself, rather than by an increase in regulatory T cells and suppression of effector T cells. *The Journal of Immunology*, 2010, 185: 1920–1926.

Interleukin-21 was discovered as a costimulatory cytokine for T cell proliferation and NK cell expansion in vitro (1, 2). IL-21 is produced by activated CD4 T cells (1), and its receptor is expressed on T, B, and NK cells (1, 3). It was also reported that IL-21 suppresses dendritic cell function (4) and increases hematopoietic progenitor cells (5). IL-21 is known to play critical roles in Ig production (6), whereas reports have differed regarding its contributions to Th1-, Th2-, and Th17-mediated effects and differentiation (6–15). IL-21 contributes to Th17 differentiation, but it may not be required for this process (7, 9, 14, 15). A relationship between IL-21 and autoimmune disease has been established. Overexpression of IL-21 induces inflammation, and in a systemic lupus erythematosus model mouse (the BXSB. 6-Yaa$^+$/J) with high serum levels of IL-21 (16), the development of disease is abrogated when these mice are crossed to IL-21R knockout (KO) mice (17). In addition, autoimmune NOD mice do not develop diabetes in the absence of IL-21 signaling (18–20).

Graft-versus-host disease (GVHD) is a major complication following hematopoietic stem cell transplantation (21), sometimes with a fatal outcome. Previously, we showed that transplantation with *IL-21R* gene-disrupted splenocytes resulted in less severe GVHD than was seen with wild type (WT) splenocytes (22). We sought to elucidate the mechanism(s) for this observation; in this article, we demonstrate dysregulated effector function of activated CD4$^+$ T cells in IL-21R$^{-/-}$ mice.

Materials and Methods

Mice

IL-21R$^{-/-}$ and IL-17$^{-/-}$ mice were generated previously (6, 23). Both were on a C57BL/6 background. Male and female mice were used as donors. C57BL/6-DBA2-F1 male mice were purchased from Clea Japan (Tokyo, Japan). All mice used in experiments were 6–12 wk old. All mice were housed in a Jichi Medical University mouse facility, which is regulated by an intramural small animal committee, and were treated in accordance with university guidelines.

In vitro T cell stimulation and MLR

Cells were cultured in RPMI 1640 (Invitrogen, Carlsbad, CA) supplemented with 10% FCS (Sigma-Aldrich, St. Louis, MO), 2 mM L-glutamine (Invitrogen), 50 μM 2-ME (Sigma-Aldrich), 0.1 mg/ml streptomycin, and 100 U/ml penicillin G (Invitrogen). Nonspecific pan T cell stimulation was performed using anti-CD3/CD28 beads for 3 d, according to the manufacturer's instructions (Dynal Biotech, Oslo, Norway). Alloantigen-specific T cell stimulation was induced by cocultivation of CD4 T cells with 30 Gy-irradiated splenocytes from C57BL/6-DBA2-F1 mice for 4 d.

GVHD models

We used IL-21R$^{-/-}$ bone marrow (BM) to eliminate the effects of WT T cells in BM. We compared transplantations with IL-21R$^{-/-}$ CD4$^+$ T cells versus WT CD4$^+$ T cells. C57BL/6-DBA2-F1 mice were irradiated with 11 Gy and injected i.v. with 5×10^6 IL-21R$^{-/-}$ BM and 5×10^6 purified CD4$^+$ T cells from WT or IL-21R$^{-/-}$ mice. The cells were purified using CD4 microbeads and AutoMACS (Miltenyi Biotec, Tokyo, Japan); the purity was >80–90%.

Pathological analysis

Two weeks after transplantation, mice were sacrificed; liver, skin, and intestine were subjected to formalin fixation, paraffin embedding, excision, and H&E staining. Photographs were taken with an Olympus BX51 microscope at ×400 magnification.

Flow cytometric analysis

Fc-block (BD Biosciences, San Jose, CA) was used to prevent nonspecific Ab binding to Fc receptors. Abs to CD4 (RM4-5), CD8 (Ly-2), CD25

*Division of Hematology, Department of Medicine, Jichi Medical University, Tochigi; †Department of Medicine and Biosystemic Science, Kyushu University Graduate School of Medical Science, Fukuoka; ‡Center for Experimental Medicine and §Frontier Research Initiative, Institute of Medical Science, University of Tokyo; ¶Animal Research Center, Tokyo Medical University, Tokyo, Japan; and ‖Laboratory of Molecular Immunology, National Heart, Lung, and Blood Institute, National Institutes of Health, Bethesda, MD 20892

Received for publication July 14, 2009. Accepted for publication May 10, 2010.

This work was supported in part by grants from the Ministry of Health, Labor and Welfare of Japan; by grants-in-aid for Scientific Research from the Ministry of Education, Culture, Sports, Science and Technology of Japan; and by the Intramural Research Program of the National Heart, Lung and Blood Institute, National Institutes of Health, Bethesda, MD.

Address correspondence and reprint requests to Dr. Katsutoshi Ozaki, Division of Hematology, Department of Medicine, Jichi Medical University, 3311-1 Yakushiji, Shimotsuke-shi, Tochigi 329-0498, Japan. E-mail address: ozakikat@jichi.ac.jp

The online version of this article contains supplemental material.

Abbreviations used in this paper: BM, bone marrow; GVHD, graft-versus-host disease; KO, knockout; Treg, regulatory T; WT, wild type.

www.jimmunol.org/cgi/doi/10.4049/jimmunol.0902217

(7D4), H-2^b (AF6-88.5), H-2^d (SF1-1.1), IFN-γ (XMG1.2), and TNF-α (MP6-XT22) were purchased from BD Biosciences, and anti-Foxp3 (FJK-16a) was from eBioscience (San Diego, CA). Intracellular staining was performed with a Cytofx/Cytoperm kit (BD Biosciences), according to the manufacturer's instructions. Cells were stimulated with anti-mouse CD3/CD28 beads for 5 h in the presence of GolgiStop (BD Biosciences). The stimulation was omitted for Foxp3 intracellular staining. An LSR flow cytometer (BD Biosciences) was used for data collection, and data were analyzed using CellQuest software (BD Biosciences).

ELISA

ELISA kits for IL-2, IL-4, and IFN-γ were from BD Biosciences, and ELISA kits for IL-21, IL-17, TNF-α, and TGF-β1 were from R&D Systems (Minneapolis, MN). Concentrations were determined according to the manufacturer's instructions.

CD25 depletion in vitro and in vivo

In vitro purification of CD4$^+$ T cells and depletion of the CD25$^+$CD4$^+$ subpopulation were performed by cell sorting using a FACSAria (BD Biosciences), which yielded highly pure populations (>98%). In vivo CD25 depletion was performed by injecting anti-CD25 Ab, as described previously (24, 25). Briefly, a hybridoma producing anti-CD25 Ab (PC61; American Type Culture Collection, Manassas, VA) was cultured in serum-free medium (Protein-Free Hybridoma Medium-II from Invitrogen), and the Ab was purified from supernatant by ammonium sulfate precipitation and a PD10 column (GE Healthcare, Buckinghamshire, U.K.). The purified product was quantified using the Bradford assay (Bio-Rad, Hercules, CA) at OD595, and 1 mg was injected i.p. weekly from day 0 for 3 wk. Control rat nonspecific IgG was purchased from Invitrogen.

Quantitative RT-PCR

At day 21 after bone marrow transplantation, CD25$^-$CD4$^+$ T cells were purified by cell sorting from recipients of WT or IL-21R$^{-/-}$ CD4$^+$ T cells; RNA was isolated (RNeasy, Qiagen, Valencia, CA), reverse transcribed using the SuperScript First-Strand Synthesis System for RT-PCR (Invitrogen), and PCR amplified using TaqMan Gene Expression Assay's primer for mouse Foxp3 (Mm00475156) and β-actin (Mm00607939) and an ABI Prism 7700 sequence detection System (Applied Biosystems, Foster City, CA).

Statistical analysis

Kaplan–Meier plots were used to compare survival rates. The log-rank test was used to evaluate p values. Statistical analyses were performed using Stat Mate ver. 6 (ATMS, Tokyo, Japan). The Student t test was used; all error bars in this study represent SD, unless otherwise specified.

Results

Purified CD4$^+$ T cell transplantation and pathological analysis

Decreased GVHD was observed when we transplanted IL-21R–deficient splenocytes compared with WT bulk splenocytes (22). Although we sought to find molecular mechanism(s) for the ameliorated GVHD, no clue was immediately evident from the transplantation experiments (22). Thus, in this study, we used purified CD4$^+$ T cells instead of bulk splenocytes in an effort to augment the differences observed. We used a well-known model of CD4$^+$ T cell-mediated GVHD (26), in which C57BL/6 mice were donors, and C57BL/6-DBA2-F1 mice were recipients. In this model, the difference between WT and IL-21R$^{-/-}$ cells seemed to be greater than in the previous experiments using bulk splenocytes (22). All recipients of WT CD4$^+$ T cells died within 55 d, whereas those receiving IL-21R$^{-/-}$ CD4$^+$ T cells survived during this time period (Fig. 1*A*). Moreover, recipients of IL-21R$^{-/-}$ CD4$^+$ T cells recovered from body weight loss by day 14, but those receiving WT CD4$^+$ T cells did not recover and continued to lose weight (Fig. 1*B*). In recipients of IL-21R$^{-/-}$ CD4$^+$ T cells, pathological analysis showed markedly reduced infiltration into the regions surrounding bile ducts and portal veins and into the interstitial region of small intestine compared with the infiltration observed in recipients of WT CD4$^+$ T cells (Fig. 2, *upper* and *middle panels*). Apoptotic bodies near the surface area of crypts in the small intestine were barely visible in recipients

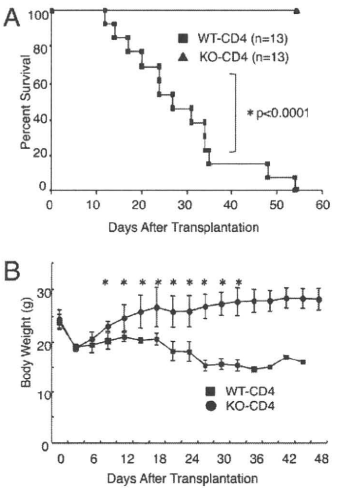

FIGURE 1. A role for IL-21 in CD4$^+$ T cell-mediated GVHD. *A*, Survival of recipients of WT and IL-21R$^{-/-}$ CD4$^+$ T cells. C57BL/6-DBA2-F1 mice were irradiated with 11 Gy and received 5 × 10^6 IL-21R$^{-/-}$ BM with 5 × 10^6 WT or IL-21R$^{-/-}$ CD4$^+$ T cells. Shown are combined data from two independent experiments. Thirteen recipients each for WT and IL-21R$^{-/-}$ CD4$^+$ T cells were analyzed. The log-rank test was used to calculate p values. *B*, Body weight after BM transplantation. Statistical significance was assessed with the Student t test.

of IL-21R$^{-/-}$ CD4$^+$ T cells, in contrast to recipients of WT CD4$^+$ T cells, in which apoptotic bodies were evident (Fig. 2, arrowheads in *middle panel*). No significant difference was observed in skin

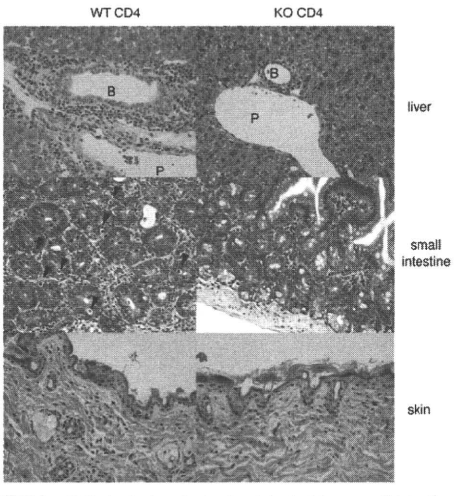

FIGURE 2. Pathological analysis of recipients. Liver, small intestine, and skin were stained with H&E (original magnification ×400). In recipients of WT CD4$^+$ T cells, cell infiltration is evident around the portal vein (P) and the bile duct (B) and into the interstitial region in small intestine. Arrowheads indicate apoptotic bodies near the surface of crypts. These changes were barely visible in recipients of IL-21R$^{-/-}$ CD4$^+$ T cells. Skin did not show any significant difference between recipients of WT and IL-21R$^{-/-}$ CD4$^+$ T cells. Shown is a representative result of six mice analyzed in each group. Only one recipient of IL-21R$^{-/-}$ CD4$^+$ T cells showed apoptotic bodies in the lumens of intestine and infiltration around the bile duct and portal vein, as was observed in the recipients of WT CD4$^+$ T cells.

pathology among recipients of WT CD4$^+$ and IL-21R$^{-/-}$ CD4$^+$ T cells. These results suggested that IL-21 might be essential for CD4-mediated GVHD, at least in this setting.

Normal cytokine production by splenocytes after transplantation is dependent on IL-21

The above observations suggested that IL-21–mediated donor CD4$^+$ T cell activation was involved in the exacerbation of GVHD. Because we could not find any significant difference in serum cytokine concentrations after transplantation (Supplemental Fig. 1), we assessed T cell differentiation by cytokine production in the presence of cellular stimulation. Interestingly, at days 14 and 21 after transplantation, bulk splenocytes from recipients of IL-21R$^{-/-}$ CD4$^+$ T cells exhibited defective cytokine production, with decreased levels of IFN-γ, TNF-α, and IL-4; in contrast, levels of IL-2, IL-17, and IL-21 were not significantly diminished (Fig. 3, *left panels*). Before transplantation, IL-21R$^{-/-}$ CD4$^+$ T cells did not show any significant defect in IFN-γ, IL-4, or TNF-α production (Fig. 3, *right panels*), suggesting that the defect was acquired after transplantation. This defect in effector T cell function might represent a mechanism for the difference in the development of GVHD by mice receiving WT versus IL-21R$^{-/-}$ CD4$^+$ T cells.

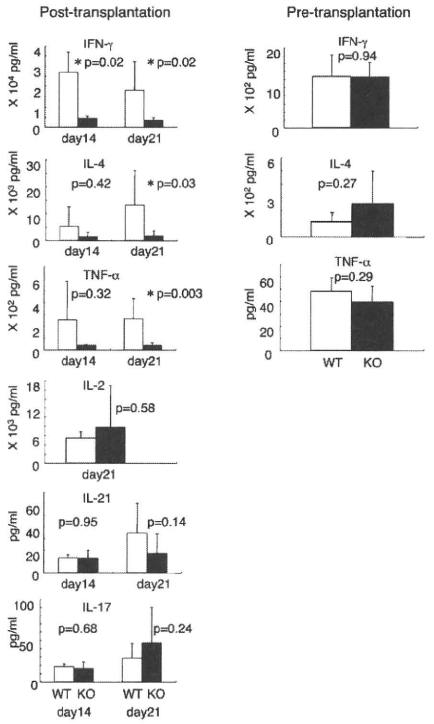

FIGURE 3. Cytokine production by bulk splenocytes before and after CD4$^+$ T cell transplantation. At days 14 and 21 after transplantation, splenocytes (5×10^5) were taken and stimulated with anti-CD3/CD28 Abs for 18 h. Concentrations of cytokines in the supernatants were determined by ELISA. Twelve or 13 recipients of WT CD4$^+$ T cells and 10 recipients of IL-21R$^{-/-}$ CD4$^+$ T cells were analyzed. Prior to transplantation, five WT and eight IL-21R$^{-/-}$ mice were analyzed. At days 14–21 after transplantation, the proportion of donor cells in the spleen was >95%. The Student *t* test was used to calculate *p* values. *Statistical significance ($p < 0.05$).

CD4$^+$ T cells were responsible for the low production of cytokines

To elucidate the basis for diminished cytokine production, we examined the number of donor CD4$^+$ T cells in the spleen at days 14–21 after transplantation. The number of donor H-2K^{d-} CD4$^+$ T cells was significantly lower in recipients of IL-21R$^{-/-}$ CD4$^+$ T cells than in recipients of WT CD4$^+$ T cells (Fig. 4*A*; $p = 0.03$, Welch *t* test; $n = 15$ versus 12), although the ranges overlapped. Because it is thought that donor T cells proliferate in secondary lymphoid organs, such as the spleen, and then infiltrate into target organs (27), the reduced number of CD4$^+$ T cells in the spleen is consistent with the reduced infiltration into the liver and small intestine, as shown above (Fig. 2). To identify the cells responsible for defective cytokine production, we performed intracellular staining and ELISA with purified CD4$^+$ T cells. After anti-CD3/CD28 stimulation, the proportion of IFN-γ$^+$ and TNF-α$^+$ cells in splenic CD4$^+$ T cells was lower in recipients of IL-21R$^{-/-}$ CD4$^+$ T cells than in those receiving WT CD4$^+$ T cells (Fig. 4*B*). Moreover, posttransplantation, the levels

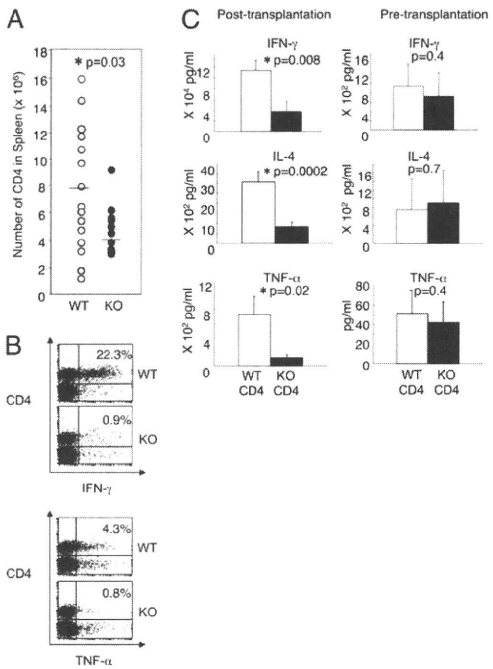

FIGURE 4. Cytokine production by splenic CD4$^+$ T cells before and after transplantation. *A*, Absolute number of donor H-2K^{d-}CD4$^+$ T cells in the spleen. The number of donor CD4$^+$ T cells was determined by multiplying the number of splenocytes by the percentage of H-2K^{d-} CD4$^+$ T cells. Each dot depicts the number of donor CD4$^+$ T cells in a mouse. Horizontal lines indicate the average. Fifteen recipients of WT CD4$^+$ T cells and 12 recipients of IL-21R$^{-/-}$ CD4$^+$ T cells were assessed. *B*, Intracellular staining of splenocytes after anti-CD3/CD28 stimulation. Splenocytes (1×10^6) were stimulated with anti-CD3/CD28 Abs for 5–6 h and stained with anti–IFN-γ or anti–TNF-α Ab in combination with anti-CD4 Ab. A total of three recipients in each group were analyzed, and a representative result is shown. *C*, Cytokine production by CD4$^+$ T cells in vitro. At days 14 or 21 after transplantation, splenic CD4$^+$ T cells (5×10^5) were purified and stimulated with anti-CD3/CD28 Abs for 18 h. Concentrations of cytokines in the supernatants were determined by ELISA. Twelve mice were analyzed in each group after transplantation. Five or six WT and eight or nine IL-21R$^{-/-}$ mice were analyzed before transplantation. *Statistical significance ($p < 0.05$).

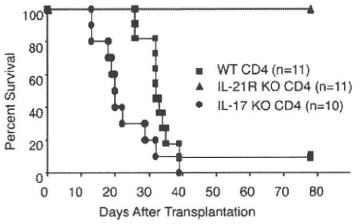

FIGURE 5. IL-17$^{-/-}$ CD4$^+$ T cells induced lethal GVHD. Survival of recipients of WT, IL-21R$^{-/-}$ (IL-21R KO), or IL-17$^{-/-}$ (IL-17 KO) CD4$^+$ T cells. Lethally irradiated (11 Gy) C57BL/6-DBA2-F1 mice were transplanted with 5×10^6 IL-21R KO BM and 5×10^6 WT, IL-21R KO, or IL-17 KO CD4$^+$ T cells. The data represent the combined results of two independent experiments.

of IFN-γ, TNF-α, and IL-4 production were significantly diminished with splenic-purified CD4$^+$ T cells from recipients of IL-21R$^{-/-}$ CD4$^+$ T cells compared with those receiving WT CD4$^+$ T cells (Fig. 4*C*, *left panels*). Before transplantation, IL-21R$^{-/-}$ CD4$^+$ T cells did not show any defect in IFN-γ, TNF-α, and IL-4 production (Fig. 4*C*, *right panels*).

IL-17 production and GVHD induced by IL-17$^{-/-}$ CD4$^+$ T cells

Although IL-21 is not essential for Th17 differentiation, IL-21 can promote it. To evaluate the effect of IL-21$^{-/-}$ CD4$^+$ T cell transplantation on IL-17 production, we measured IL-17 after transplantation. As shown in Fig 3, *bottom left panel*, bulk splenocytes from recipients of IL-21R$^{-/-}$ CD4$^+$ T cells produced comparable amounts of IL-17 at days 14 and 21 after transplantation compared with mice receiving WT CD4$^+$ T cells. Moreover, we found that IL-17$^{-/-}$ CD4$^+$ T cells induced lethal GVHD analogous to WT CD4$^+$ T cells (if anything, death occurred earlier), suggesting that IL-17 is dispensable for this process, in contrast to the essential role of IL-21, as reflected by the survival of mice receiving IL-21R$^{-/-}$ CD4$^+$ T cells (Fig. 5).

Regulatory T cell number in spleen

We next determined the serum concentration of the major immunosuppressive cytokine, TGF-β1, at days 6–21 after transplantation. We found an increase in TGF-β1 only after transplantation (Fig. 6*A*; $p = 0.0003$ at day 14; $p = 0.01$ at day 21, Student t test). In splenocytes from recipients of IL-21R$^{-/-}$ CD4$^+$ T cells, the production of TGF-β1 and IL-10 by in vitro T cell stimulation was not upregulated; in fact, it tended to be diminished (Supplemental Fig. 2), suggesting that the increase in serum TGF-β1 might be due to cells other than T cells. Because naive T cells can differentiate into regulatory T (Treg) cells in the presence of TGF-β1 (28), and it was reported that IL-21$^{-/-}$ T cells were predisposed to differentiate into Treg cells (8), we also investigated whether more Treg cells were induced in recipients of IL-21R$^{-/-}$ CD4$^+$ T cells. The proportion

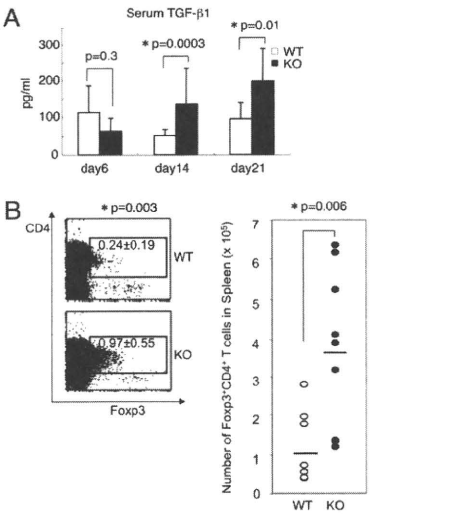

FIGURE 6. Increase in splenic Treg cells. *A*, Upregulation of serum TGF-β1. Serum TGF-β1 concentrations at the indicated day after transplantation were determined by ELISA. Three samples from recipients of WT CD4$^+$ T cells and 4 samples from recipients of IL-21R$^{-/-}$ CD4$^+$ T cells at day 6, 23 samples from recipients of WT CD4$^+$ T cells and 25 samples from recipients of IL-21R$^{-/-}$ CD4$^+$ T cells at day 14, and 8 samples from recipients of WT CD4$^+$ T cells and 7 samples from recipients of IL-21R$^{-/-}$ CD4$^+$ T cells at day 21 were analyzed. *Statistical significance ($p < 0.05$). *B*, The percentage and absolute number of splenic Foxp3$^+$CD4$^+$ regulatory T cells at day 14 after transplantation. The left panel shows a representative flow cytometric result from eight or nine similar samples. The right panel indicates the number of all samples; the averages are indicated by the horizontal lines.

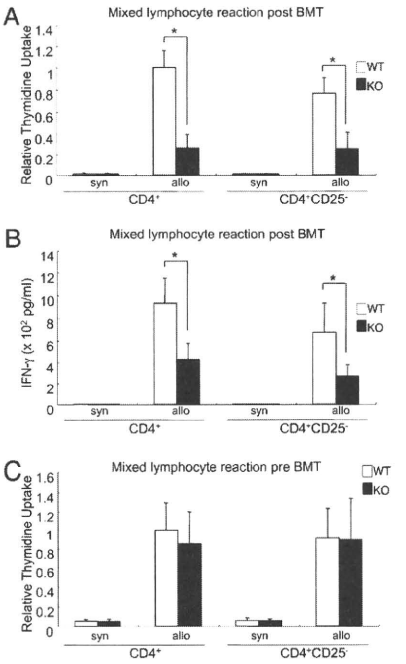

FIGURE 7. An impaired CD4 alloreaction is not dependent on CD25$^+$ CD4$^+$ T cells. CD4 alloreaction in vitro was impaired after transplantation, and this impairment was not restored by CD25$^+$ T cell depletion. *A*, At day 14 after transplantation, 1×10^5 sorter-purified splenic CD4$^+$ or CD25$^-$ CD4$^+$ T cells (>98% purity) were cultured with 4×10^5 irradiated allogeneic C57BL/6-DBA2-F1 splenocytes for 4 d. The cells were pulsed with 1 μCi of [^{3}H]thymidine for the last 24 h. Relative thymidine uptake to the value of WT CD4$^+$ T cells is depicted. *B*, Culture was the same as in *A*, but IFN-γ concentrations in the supernatants were determined by ELISA. *C*, Sorter-purified splenic CD4$^+$ or CD25$^-$CD4$^+$ cells from nontransplanted mice were cultured with irradiated allogeneic C57BL/6-DBA2-F1 splenocytes. Relative thymidine uptake to the number of WT CD4$^+$ T cells is depicted. *$p < 0.05$.